Alpaca Polyclonal IgG Antibodies Protect Against Lethal *Andes Virus* Infection

by

Patrycja Magdalena Sroga

A thesis submitted to the Faculty of Graduate Studies of

The University of Manitoba

In partial fulfillment of the requirements of the degree of

Master of Science

Department of Medical Microbiology and Infectious Diseases

University of Manitoba

Winnipeg

Abstract

Hantaviruses remain a global health issue as the number of infections continues to rise from year to year. *Andes* virus (ANDV), a South American *Hantavirus* strain carried by the long-tailed pygmy rice rat *Oligoryzomys longicaudatus*, causes over 200 infections each year in Argentina and Chile. The virus is transmitted through inhalation of infected rodent excreta, however numerous reports have confirmed person-to-person cases as well. ANDV is responsible for causing Hantavirus Pulmonary Syndrome and the lack of an approved therapeutic and/or vaccine is a problem as the fatality rate ranges from 30-50% between outbreaks. Recent animal studies have documented the potential of using antibodies as an effective treatment for *Andes* virus infections. The central hypothesis of this thesis is that neutralizing alpaca IgG antibodies produced through DNA vaccination will provide protection against lethal ANDV challenge within the Golden Syrian hamster model. This hypothesis was addressed by vaccinating alpacas and generating hyperimmune *Andes* virus-specific polyclonal IgG antibodies. Afterwards, these antibodies were evaluated in a bioavailability and protection study within the lethal Golden Syrian hamster model. Purified neutralizing polyclonal IgG alpaca antibodies were found to be 100% protective against lethal ANDV hamster infection when administered at days +1 and +3 post challenge. The success of this study provides promising proof of concept data that neutralizing alpaca PcIgG antibodies have the potential to be a highly effective and novel treatment for ANDV infections.

Dedication

This thesis is dedicated to my parents, Barbara and Norbert, and brother, Thomas. Thank you for your love, support, and encouragement to pursue my dreams.

Acknowledgements

First and foremost I would like to thank my supervisors Dr. Michael Drebot and Dr. David Safronetz for the opportunity to work within the Special Pathogens group. With your guidance and support, I have gained not only the skills but the confidence to challenge myself in regards to research.

I would also like to thank my committee members, Dr. Blake Ball and Dr. Janilyn Arsenio. Thank you for your enthusiasm and support throughout this journey.

I would like to thank Dr. Darryl Falzarano and the Veterinary team at VIDO-Intervac/ University of Saskatchewan for the opportunity to collaborate, as well as their expertise throughout this project. Thank you to Angela Nelson and the Department of Medical Microbiology for your constant support and guidance throughout this journey. Thank you to my fellow graduate students and close friends Jasmine Frost and Lauren Garnett, for the numerous coffee pick-me-ups and the chance to vent following failed experiments.

Thank you to my fellow lab members, Derek, Bryce, Angela, Yvonne, Geoff, Rob, and the entire Special Pathogens team. Thank you for your friendship and always being there to help.

Finally, thank you to my friends and family for always supporting me. I am incredibly lucky to have such wonderful people in my life.

Table of Contents

List of Tables

List of Figures

Chapter 1. Introduction

1.1 Origin and Early History of Hantaviruses

1.1.1 Old World Hantaviruses and HFRS

The symptoms and signs of hemorrhagic fever with renal syndrome (HFRS) have been known to Chinese and Eastern European physicians since the 1930's, although the earliest documentation of a similar disease dates back to the Chinese Western Zhou dynasty, roughly 1000 AD [1]. During World War 2, Japanese soldiers were commonly affected by cases of nephritis and bouts of fever, which lead to increased efforts to identify the cause of the yet unknown disease [1,2]. It wasn't until the early 1950's Korean War that the severity of the disease, then known as Korean hemorrhagic fever, was seen on a mass scale [1,3,4]. This first major outbreak affected more than 3000 United Nations troops who displayed symptoms of shock, renal failure, and fever, with an average mortality rate of 10-15% [1,3–6]. From then, Western scientists began investigating the causative agent and in 1977 the viral antigen was identified in the Korean rodent *Apodemus agrarius* from a positive reaction using sera from HFRS-affected individuals [1,3,6]. The isolated virus was named Hantaan virus (HNTV), after the river in North and South Korea where numerous cases were documented during the Korean War [1,3].

Since the discovery of HNTV in 1977, numerous Old World Hanta species have since been identified across Europe and Asia [1,3]. Since the early 1930's, cases of 'Nephropathia Epidemica' (NE) were common in soldiers across Sweden and Finland [1,3]. In the 1980's, the now-known Puumala virus (PUUV) was isolated from the rodent *Clethrionomys glareolus* and was proven to be a relative of HNTV [1,3]. This was followed by the

isolation and discovery of Seoul virus (SEOV), Dobrava virus (DOBV), and roughly 8 other Old World Hantavirus species [6]. To pinpoint the exact origin of these negative-sense RNA viruses is difficult, however sequencing analysis suggests that Old World Hantaviruses in Asia have evolved over thousands of years within their rodent *Murinae* and *Arvicolinae* families [6–8].

Old World Hantaviruses are characteristic for causing HFRS, a disease ultimately resulting in renal failure [6]. Transmission of old world hantaviruses occurs through inhalation of contaminated rodent urine, feces, and saliva, with a typical incubation period of roughly 2 to 4 weeks [6,9]. After viral transmission HFRS progresses through five phases, the first being the febrile phase [6,9]. The symptoms experienced within this phase are common to a variety of illnesses and diseases such as fever, malaise, chills, nausea, and vomiting caused by hypotension [4,6,9,10]. This period typically lasts 3 to 7 days, with blurred vision and areas of facial hemorrhage occurring towards the end of the phase [4,6,9,10]. The second phase, hypotensive phase, quickly begins and can last hours to several days [4,6,9,10]. The characteristic symptoms include hypotension due to vascular leakage, nausea, vomiting, tachycardia, and shock [4,6]. Shock is a particular life-threatening symptom, ultimately causing approximately one third of all HFRS deaths [4,6]. Vascular leakage introduces additional life-threatening symptoms such as thrombocytopenia, haematuria, and cranial hemorrhage,s causing impaired mental function [4,6]. The third phase of HFRS, oliguric phase, lasts up to two weeks and is primarily characterized by the onset of oliguria or low urine output [4,6]. Oliguria occurs as a result of impaired kidney function or onset of kidney failure, leading to additional symptoms of proteinuria, shock,

increased hemorrhages, and severe back pain [4,6]. As kidney function continues to decrease, approximately one-third of patients are placed on dialysis [4,6]. The oliguric phase is often considered the most dangerous phase as approximately one half of deaths occur during this period of the disease course [4,6,10]. However, individuals who progress to the fourth stage of the disease begin to show signs of recovery [6]. Patients in the polyuric phase display increased kidney function and increased urine output, lasting a period of several weeks. In the final phase, convalescent phase, patients typically undergo a complete recovery and kidney function returns to normal [4,6]. However, long term complications such as hypertension and chronic renal failure develops in a small group of affected individuals [4,6].

Old World Hantaviruses continue to remain a global problem as more than 100,000 cases are reported each year [6,11]. Although the symptoms of disease remain similar among Old World Hantaviruses, fatality rates, number of affected individuals, and severity of HFRS differs based on the identity of the causative agent. Cases of Hantaan virus (HNTV) infections, transmitted by the field mouse *Apodemus agrarius*, are typically concentrated within China, Russia, and South Korea [4,6]. HNTV is identified as one of the more severe HFRS-causing viruses, causing thousands of cases per year with fatality rates up to 10% [4,11]. Affected individuals commonly experience the more severe symptoms associated with HFRS, such as internal hemorrhages and hypotension [4,11,12]. Dobrava-Belgrade virus (DOBV), transmitted by *Apodemus flavicollis* and found in the Balkans, is an additional Old World Hantavirus associated with more severe symptoms and higher mortality rates (5-12%) [5,6,10]. In contrast, Seoul virus (SEOV), transmitted by the

Norway rat *Rattus norvegicus* and found globally, causes death in less than 1% and is commonly associated with symptoms of headache, nausea, and proteinuria [6,13]. A mild form of HFRS, nephropathia epidemica (NE), is also seen across Europe and Asia as a result of Puumala virus (PUUV) transmitted by the vole *Clethrionomys glareolus* [6,14].

1.1.2 New World Hantaviruses and HPS/ HCPS

In contrast to Old World Hantaviruses, the discovery of New World Hantaviruses began in the early 1990's with the North American *Sin Nombre* virus [6,15,16]. During the late spring of 1993, a young man of Native American ancestry was examined by a physician in New Mexico, USA due to complaints of fever and myalgia [15,16]. As his symptoms did not pose any dangerous warning signs, he was treated and released from medical care [15,16]. However, several days later his condition worsened with the individual exhibiting severe shortness of breath [6,16]. The young man collapsed and was immediately rushed to hospital due to respiratory failure, where he ultimately died due to unsuccessful resuscitation attempts [6,16]. This case alarmed the state authorities as the facility had witnessed a similar incident involving a young woman just a few weeks earlier [6,16]. The cases seemed to cluster around a Navajo town in New Mexico, with signs of respiratory failure and pulmonary edema prevalent in both fatalities [6,16]. A health emergency was issued in the Four Corners Area (New Mexico, Utah, Arizona, Colorado) and 30 additional cases were identified, all having exhibited the same signs and symptoms [6,16]. Shortly after the emergency was issued, the unknown virus and host were identified as *Sin Nombre* virus, a novel hantavirus, carried by the deer mouse *Peromyscus maniculatus* [3,6,16]. The discovery came as a surprise to scientists as at that time there were no known North

American hantaviruses causing disease in humans [3,16]. It is generally believed that the outbreak occurred as a result of the increased moisture within the area due to the El Niño winter, bringing an abundance of vegetation and thus attracting a larger population of deer mice [3,16].

The discovery of SNV and Hantavirus Pulmonary Syndrome (HPS) was a turning point for scientists and clinicians as possible New World Hantavirus cases could now be accurately identified. This knowledge eventually led to the identification of additional North American Hantavirus strains including: Bayou virus, carried by the Louisiana rat *Oryzomys palustris*, New York virus, carried by the deer mouse *Peromyscus leucopus*, and Black Creek Canal virus, carried by the Florida rat *Sigmodon hispidus* [3,6,17]. In addition to North American cases, numerous cases of HPS-like disease have been reported in South America, including Paraguay, Argentina, and Chile [6,10,18]. An outbreak of Hantavirus, later identified as Laguna Negra virus, resulted in the death of 17 people, several who were healthy young individuals [6,18]. Andes virus, mostly confined within Argentina and Chile, was responsible for an outbreak in the Andes Mountains in 1996 [6,18]. Choclo virus (CHOV), carried by *Oligoryzomus fulvescens*, is commonly prevalent in Panama, having been responsible for over 150 cases and 30 fatalities from HPS since 2000 [6,19]. Since surveillance began in the early 90's, fatalities from over 15 different South American Hantavirus strains have been documented [6,20]. As with Old World Hantaviruses, the origin of Hantavirus in the Americas is still unknown [7,8,20]. Rodents of the New World Hantaviruses belong to the *Sigmodontinae* family, sharing a common ancestor with the Old World *Murinae* family approximately 30 million years ago [7,20]. There is conflicting data

regarding the exact date of Hantavirus emergence as well as the evolution of each virus [7,20]. However, studies suggest that these viruses have evolved alongside their hosts, ultimately giving rise to the numerous strains we know of today [7,20].

Hantavirus Pulmonary Syndrome (HPS), additionally known as Hantavirus Cardio-Pulmonary Syndrome (HCPS), is the disease associated with New World Hantavirus infections [6]. While there are over 100,000 cases of HFRS each year, up to a thousand cases of HPS are reported yearly, majority occurring within South America [6,21]. However, fatality rates are much higher with HPS, averaging 30-50% [6,21]. As with Old World hantaviruses, New World hantaviruses are transmitted through inhalation of contaminated rodent excreta or through bites, however *Andes* virus has also been documented to transmit from person-to-person [6,10,20,21]. Initial symptoms of HPS (prodrome phase) begin anywhere from 1 week to 4 weeks post exposure, with affected individuals experiencing high fever, malaise, vomiting, and intense abdominal pain [6,10,20,22]. The cardiopulmonary phase begins roughly 5 days after the commencement of the prodrome phase, with coughing and shortness of breath as the initial symptoms [6,10,20,22,23]. The cardiopulmonary phase is the most dangerous stage as the full effects of capillary leakage are observed, including pulmonary edema, parenchymal infiltrates, tachycardia, shock, and thrombocytopenia [6,16,23]. Individuals in this stage of the disease often require mechanical ventilation systems or extracorporeal membrane oxygenation as a result of heart and lung failure [6,16,23]. About 40% of individuals with HPS die in this phase, however those who progress to the convalescent phase of the disease typically complete a full recovery [6,16,23]. In the convalescent phase individuals typically regain

pulmonary function and normal urine output following diuresis [6,16,23]. There is currently no evidence of disease recurrence or severe long-term effects for individuals who have completed a full recovery from HPS [6,10,16,23]

1.2 Phylogeny and Transmission Routes of Hantaviruses

Hantaviruses, both Old and New World, are primarily transmitted by rodents [24–26]. Individuals become infected through direct contact/inhalation of contaminated rodent excreta or through bites by the host, however there have been documented cases of person-to-person transmission with ANDV [24–26]. With HFRS, the hosts include field mice and rats across China and Europe, while HPS cases are primarily caused by deer mice for SNV and the pygmy rice rat for ANDV [24–26]. The typical reason for the separation of Old and New World Hantaviruses stems from not only their respective diseases, but also from the hosts that carry them [24–26]. As mentioned previously, the Old World Hantavirus hosts belong to the *Murinae* and *Arvicolinae* subfamilies, while the New World Hantavirus hosts belong to the *Neotominae* and *Sigmodontinae* subfamilies [24–26]. The average difference within the hanta genome **(Figure 1)** between rodent hosts is roughly 20-30% for the S, M, and L segments [25].

Although rodents were considered to be the only Hantavirus hosts for many decades, discoveries of new Hantavirus species have expanded the host range to include other mammalian species such as bats, shrews, and moles [24–26]. The discovery of African hantaviruses such as *Tanganya* virus found in Chiroptera bats have brought the origin and evolution of hantaviruses into question amongst the scientific community [21,27]. In 2006

a new Hantavirus species *Magboi* virus was identified in bat lung tissue from Sierra Leone. This discovery came as a surprise as previous Hantavirus discoveries in bats were a result of laboratory contamination and not natural infection [21,27]. Until recently it was largely hypothesized that current Hantaviruses have resulted from the divergence from a common ancestor with years of evolution occurring within their respective hosts [21,25,26]. With the discovery of Hantaviruses in shrews and bats, the initial perception or explanation was that spill-over events had occurred due to environmental or evolutionary pressures, most commonly a result of increased encounters between species [21,25,26]. This event would lead to eventual 'host-switching' and divergence of viruses over time, leading to the diverse group of viruses and hosts we see today within the *Hantaviridae* family [21,25]. However, there is mounting evidence that points away from this theory, revealing that Hantaviruses do not indeed share a single common ancestor [21,25]. In fact, phylogenetic analysis suggests that Hantaviruses originate from several ancestral viruses that continued to exchange with each other and within several mammalian hosts over time [21,25]. Different environmental and evolutionary forces continued to shape these viruses in a variety of hosts, including over 50 rodents, 7 bats, and almost two dozen moles and shrews [21]. Although the origin of Hantaviruses may be somewhat clearer, the time line of these exchanges and evolutionary events is still debatable [21,25].

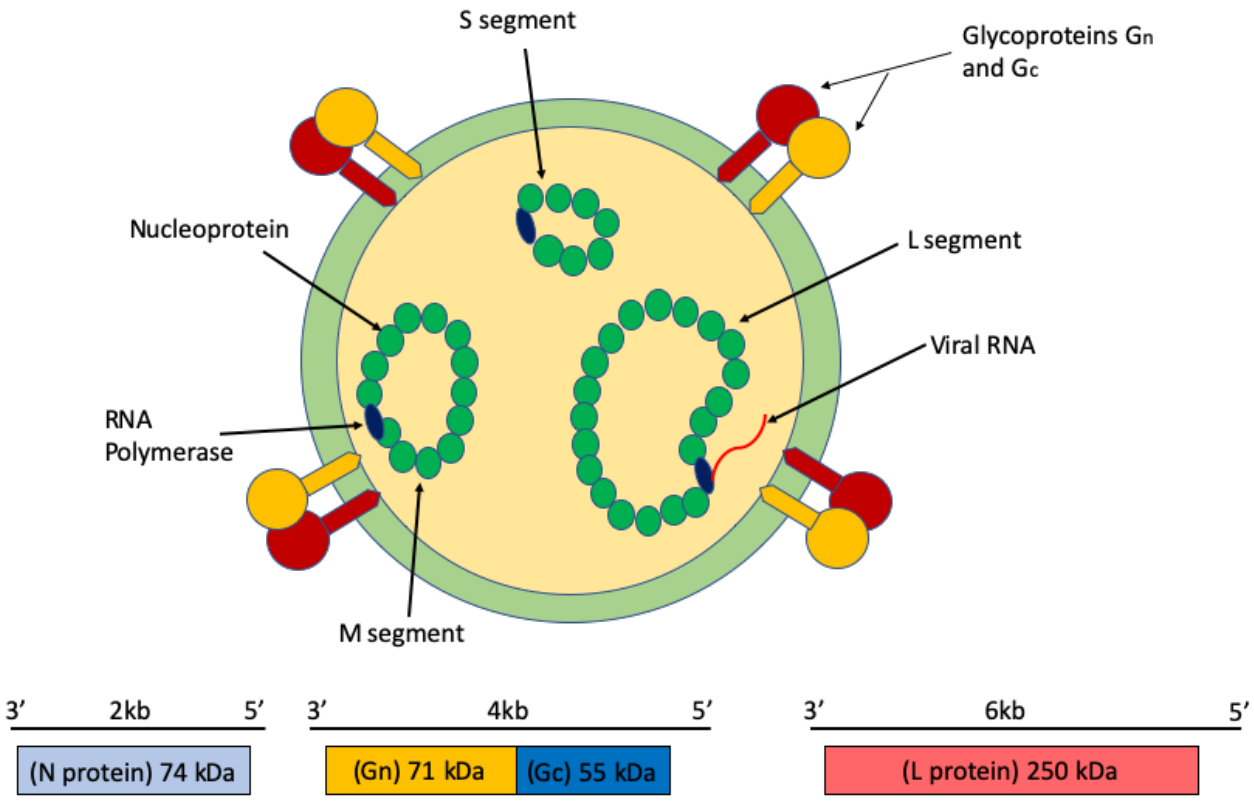

Figure 1. Structure of ANDV and viral protein sizes (S, M, L segments).

1.3 History of Andes Virus Outbreaks

The emergence of *Andes* virus (ANDV), belonging to the New World Hantavirus family, can be traced back to the mid-90's with the first ever reported case(s) occurring in Argentina [28,29]. Sporadic cases of individuals succumbing to severe respiratory illness were documented in rural communities in both central and western Argentina, including a family outbreak in El Bolson, rural western Argentina, in the spring of 1995 [28,29]. Here 3 affected individuals contracted an unknown respiratory illness, ultimately resulting in 2 unexplained deaths [28,29]. When serology was performed using the patient serum samples, it was discovered that the serum contained IgG and IgM antibodies that cross-reacted to *Sin Nombre* virus (SNV), a member of the New World Hantavirus family [28,29]. Using RNA extracted from infected tissues, sequencing analysis revealed that a new Hantavirus, ANDV, was the causative agent [28,29].

Since the initial identification and characterization of ANDV in 1995, there have been reports of multiple ANDV cases and outbreaks across Argentina and Chile [28–31]. Just one year after the initial cases in El Bolson, over a dozen more individuals contracted the virus, including three physicians who became ill after coming in contact with infected individuals [6,32]. Between 1997 and 1998 an outbreak of HPS was reported in southern Chile when over two dozen individuals became ill [6,28,33]. The outbreak occurred in three waves, the first of which began in July 1997 when a 39-year old male died from severe respiratory distress several days after onset of symptoms [6,33]. The spouse and two children of the affected individual became ill with HPS several weeks after, with the mother ultimately dying from respiratory failure [6,33]. Additionally, the brother-in-law and sister-

in-law of the family became ill and both died several weeks later after visiting the household [6,33]. Confirmation of ANDV as the etiological agent was done using reverse-transcriptase PCR (RT-PCR) and serology in all affected individuals [6,33]. The second wave of the outbreak occurred in the Aysen region of Chile in 1997 in which 5 family members became ill with HPS [6,33]. Lastly, the third wave of the outbreak occurred in December of the same year after the male head of a family in southern rural Chile died from HPS-suggestive respiratory distress [6,33]. Shortly after, his wife began exhibiting symptoms but luckily survived the disease course [6,33].

Although the initial outbreaks of ANDV occurred in rural areas, a large number of cases have been reported in urban settings since 2000 [6,28,34]. From 2000 to 2007 over 400 cases of HPS have been documented across different regions in Chile, with an average mortality rate of 40% (Jonsson et al., 2010; Martinez-Valdebenito et al., 2014; Medina et al., 2009);Jiang, Du, Wang, Wang, & Bai, 2016). Over 100 cases of HPS are reported each year in Argentina with a similar mortality rate [6,28,30]. As of recently, more than 800 cases of HPS have been documented in Chile [6,28,30]. It is typically seen that a fair majority of cases occur between family members, indicating that person-to-person transmission is an important factor in regards to the spread of the virus. [28,30,34,36].

1.4 Andes Virus Structure and Replication

1.4.1 ANDV Structure

Andes virus, as with all members of the *Hantaviridae* family, possesses a negative-sensed single stranded (ss) RNA genome, a unique feature common to all members of the *Bunyavirales* order [37,38]. The viral RNA is tri-segmented (**Figure 1)**, meaning that its open-reading frame regions are separated into three distinct units: a small (S) segment of 2kb that encodes the nucleocapsid protein (N), a medium (M) segment of 4kb that encodes the glycoprotein precursor (GPC), and the large (L) segment of 6kb that encodes the RNA-dependent RNA polymerase [37,38]. The ends of each segment of RNA are highly conserved and complementary to each other, allowing for the formation of a structure that is predicted to act as the promoter [39–41].

The S segment encodes the viral nucleocapsid protein which is responsible for binding viral RNA and forming viral ribonucleoproteins (RNP's), functioning to protect the genome from enzymatic degradation [39–41]. It is not completely understood how the formation of RNP's occur, but it is strongly hypothesized that the S segment is able to interact with the 'panhandle' structure formed by the non-coding complementary ends of viral RNA, leaving the mRNA free [39–41]. In some Hantaviruses, as seen with ANDV, the S segment encodes an additional protein called the non-structural protein (NSs) that is located downstream from the N protein open-reading frame [39–41]. It is suggested that translation of the NSs region occurs through a 'leaky scanning' mechanism following translation of the N coding regions [39–41]. The NSs plays a role in viral infection, involved in down regulation of host immune responses [39,41]. The M segment encodes

the GPC, an 1130-1160 amino acid protein precursor, that is eventually cleaved to produce the surface glycoproteins G_n (N-terminus) and G_c (C-terminus), previously known as GP_1 and GP_2 [37,41]. Translational cleavage of the GPC occurs at a unique site within the C-terminus of the G_n glycoprotein called the WAASA sequence (amino acids 644-648), where peptidases are signalled to initiate cleavage [37,41]. The glycoproteins are assembled into a spike complex, each consisting of four G_n and four G_c units, that protrude out of the viral lipid membrane at approximately 10nm [37,41]. Both glycoproteins have a large globular body situated outside of the virion lipid envelope, and an internal C-terminus tail located within the virion structure that is connected to the body through a transmembrane hydrophobic helix [37,41]. Finally, the L segment encodes the roughly 250kDa viral RNA-dependent RNA polymerase [6,37,41]. With each piece of the genome playing an important role, the overall virion structure is a sphere of roughly 120nm in diameter consisting of a lipid envelope studded with glycoprotein heterodimer spikes encompassing the S, M, and L segments of the hanta genome within the virion [6,37,41].

1.4.2 ANDV Replication Cycle

The replication cycle of ANDV begins with cellular entry, involving the essential glycoprotein spike complexes embedded within the lipid envelope of the virion particle [42,43]. The virus replicates within vascular endothelial cells, found abundantly in the lungs and kidneys, with the initial contact occurring between the surface glycoproteins and integrin receptors, which play an important role in cell to cell adhesion [41,44,45]. It is important to distinguish that pathogenic Hantaviruses interact with $\alpha_v\beta3$ receptors, whereas non-pathogenic hantaviruses interact with $\alpha5\beta1$ integrin receptors [38].

Interaction between the surface glycoproteins and Protocadherin-1, a membrane protein expressed in airway epithelial cells, is also essential for New World Hantaviruses [44]. There have been multiple other cell receptors described regarding Hantavirus entry, including β1 integrins, decay-accelerating factor DAF, and complement C1q receptors, however how and whether they are actually involved in cell entry is yet to be determined [38,41,46].

Once the virus-cell interaction has been established, the virus enters the cell through endocytosis [37,38]. Hantaviruses can enter via a clathrin-mediated pathway resulting in a clathrin vesicle encapsulating the virion, however not all Hantaviruses, such as ANDV, use this method [37,38]. Alternative entry routes are proposed to involve macropinocytosis and cholesterol-dependent endocytosis [37,38,41]. Following viral entry into the cell, the virion travels through the cell within an early endosome that matures to a late endosome after an essential pH change [37,38,41]. The reduction of pH from the early to the late endosome is essential for successful viral replication, as the low pH causes conformational changes within the glycoprotein complex which ultimately allows for the fusion of both the viral and endosomal membranes [38,41,46]. The RNP's are now free within the cytoplasm, where they are transported to the endoplasmic reticulum for viral replication [46]. The Hantavirus negative-sensed ssRNA is transcribed into viral mRNA by the viral RNA-dependent RNA polymerase [37,38,43]. A 5'cap is necessary for translation of mRNA to protein to occur, which is done by a process called 'cap snatching' where caps are stolen from host mRNAs [37,38,43]. In addition to transcription, the viral genome must be replicated in order to produce more virus particles. This process involves transcription of

viral RNA to complementary RNA (cRNA), where the cRNA can serve as a template for replication [37,38,43]. Viral replication is unique in that it does not require a 5'cap. The vRNA eventually binds with the viral nucleoproteins to make RNP's after the 3' and 5' complementary ends form the 'panhandle' structure [37,38,43]. The exact locations of each replication step remains a mystery, however it is believed that replication occurs in distinct Endoplasmic Reticulum-Golgi complexes which eventually bud off the Golgi to form naïve virus particles [37,38,43]. Before budding occurs, the M segment of the viral genome is translated within the endoplasmic reticulum to form the G_n and G_c glycoproteins and transported to the Golgi for glycosylation [37,38,43]. The virion assembles, buds from the Golgi, is transported to the plasma membrane of the host cell, and a mature virion is released from the cell through exocytosis [37,38,43]. Not all Hantaviruses assemble at the Golgi, such as SNV which has been proposed to also assemble at the plasma membrane [37,38,43].

1.5 Andes Virus Transmission and Pathogenesis

1.5.1 Person-to-Person Transmission of ANDV

As with all pathogenic Hantaviruses, human transmission of ANDV typically occurs through inhalation of virus particles from infected rodent urine and feces, as well as bites from an infected rodent host [30,32]. The virus can survive in the environment for several weeks and additionally can transmit from person-to-person [30,32]. Similarly, Crimean-Congo Hemorrhagic Fever can be transmitted between individuals through direct contact with infected blood or bodily fluids [47]. The information regarding these cases is rare with respect to ANDV, as only about 100 cases total are reported per year [30,33,48].

Regardless, confirmed person-to-person cases show similarities, most importantly being that it is usually family members and/or healthcare workers that are affected [30,33,48]. The first major outbreak of ANDV in 1996 involved 20 individuals that were either residents or visitors of a rural community in southern Argentina [32,48,49]. Among those affected included 5 medical workers, all of which had never travelled to the rural community and began exhibiting symptoms of HPS only after direct contact with an infected individual [32,48,49]. In addition, the outbreak was centered around 2-3 families where individuals became sick after direct contact with an infected host or contact with an infected family member [32,48,49]. An in-depth sequencing analysis of the virus was performed from each patient using blood and tissue samples of which RNA was extracted and amplified through reverse-transcriptase PCR [29,32]. The criteria used during this analysis was the similarity of sequences, where an exact match of 500 nucleotides or more between samples strongly suggested that person-to-person transmission had occurred [29,32]. The results indicated strong sequence similarity between samples with less than 9% difference in the S and M sequences between cases [29,32].

The first major outbreak of HPS in Chile occurred just one year after the Argentinian outbreak [49]. After years of sporadic and random cases, in 1997 numerous cases of HPS were identified in the Aysen region of Chile [49]. This outbreak displayed similar features as the Argentinian outbreak, such as affecting primarily family members and affecting individuals of all ages [49]. Overall almost a dozen people were infected, and 55% died [49]. The outbreak sparked particular interest as the families who were affected lived in an area near Argentina where cases of person-to-person transmission were previously seen

[49]. However, investigation of hospital workers and individuals who came into close contact with affected persons showed no evidence of person-to-person transmission occurring in this region, despite healthcare workers ignoring transmission personal protective equipment (PPE) precautionary measures [49]. A unique finding in the study was that 12 of the 319 participants tested positive for ANDV IgG within the affected region [49]. A recent outbreak in 2010 occurred in yet another small community in Chile, affecting 5 individuals [30]. As with previous person-to-person ANDV outbreaks, those affected were family members as well as healthcare workers who became ill after close contact [30]. This outbreak is the first one that documents accounts of nosocomial transmission, as secondary individuals only became ill after coming into close contact with infected bodily fluids [30].

Although person-to-person transmission cases are uncommon and difficult to pinpoint, they generally demonstrate similarities such as occurring within family clusters, affecting healthcare workers, and most importantly occurring as a result of direct contact with an infected individual and infected bodily fluids such as saliva and urine [30]. As ANDV RNA has been found in various secretions including urine, it is speculated that transmission between individuals is commonly caused through inhalation of droplets or aerosolization of virus through various methods including intubation and changing of contaminated beddings [32,50]. Although ANDV is the only Hantavirus species that demonstrates person-to-person transmission there is fear that global warming will lead to larger outbreaks in more densely populated areas.

1.5.2 Pathogenesis of HPS/HCPS

The severe and life threatening complications from HPS all stem from vascular leakage, which is characteristic for both New World and Old World Hantavirus infections [51,52]. The virus primarily infects pulmonary endothelial cells and, understandably, the lungs are the targeted organ as it contains a vast amount of this cell type [51–54]. The mechanism of action is still not entirely defined, however the virus does not cause cell lysis which suggests that modulation of the immune system plays a significant part in disease progression [52,53]. As mentioned previously, the virus binds to host cells through the interaction of viral surface glycoproteins with host cell surface receptors, such as β3 integrins located on endothelial, epithelial, and macrophage cells [51,52]. Once inside the cell, the virus is recognized by macrophages and dendritic cells which respond by activating pro-inflammatory pathways, increasing production and release of inflammatory cytokines such as interleukin-6 (IL-6) for T cell differentiation and B cell stimulation, and interferon-gamma (IFN-γ) for macrophage stimulation, to the area [51,52]. The body responds by activating these pro-inflammatory pathways in order to help with pathogen clearance, however ANDV exploits these pathways to its advantage [51,52]. The ultimate decrease or loss in membrane function is attributed to multiple factors. First, levels of vascular endothelial growth factor (VEGF) increase as a result of infection [52,55]. VEGF is involved in the production of new vasculature for the human body and increased vascular permeability is a result of this process [52,55]. Second, coagulation abnormalities occur possibly due to a decrease in platelets and other factors, however this process is yet to be understood for HPS [52]. It is speculated that the virus is able to evade host protective mechanisms such as Human MxA/B protein that interacts and inhibits RNA viruses [56].

In this circumstance, ANDV has been shown to interact with MxA/B resulting in a delay in the IFN-β pathway, a pathway responsible for multiple actions such as decreasing pro-inflammatory cytokine production [57]. However, further studies are needed in order to pinpoint exactly how the virus alters these mechanisms *in vivo*. The ultimate changes and evasion of the host immune system are important for virus propagation and disease spread, as there is a correlation between levels of viral RNA and severity of disease within the individual [54].

ANDV has been shown to interact with cytotoxic (CD8+) T cells as they ultimately recruit them to the lungs during HPS [52,53]. Post-mortem analysis has shown that infiltrates in the lungs of HPS individuals are composed of a large number of cytotoxic T cells (CD8+), suggesting that these cells are involved with the progression of disease [52,53]. T cells are responsible for fighting foreign pathogens either through direct killing mechanisms or through recruitment of host immune factors and cells. There is no evidence showing that ANDV-infected cells are directly killed by T cells, but rather that these cells are manipulated by ANDV to attract additional pro-inflammatory factors to the area which in turn ultimately results in impaired vascular membrane function [52,53]. One topic of interest has been whether or not there is a correlation between disease severity and having certain genes [58]. Regarding T cells, individuals with certain haplotypes of the T cell receptor Human Leukocyte Antigen (HLA) display a more severe disease course than those with other haplotypes [58]. In particular, individuals with type HLA-B08 displayed a severe form of HPS while those with HLA-DRB115 had a milder form of the disease [58]. The exact reasoning behind these differences is not yet confirmed [58]. Interestingly,

although T cells play an important role in the spread of disease in humans, they do not correlate with the severity of disease in the lethal Syrian hamster model [53,58].

1.6 Vaccines and Treatments for HPS/HCPS

1.6.1 Diagnosis, Vaccines, and Antivirals

Diagnosis of ANDV cases involves examining the clinical signs and symptoms of the patient, as well as evaluating the information presented through serology or molecular-based testing [59]. The clinical signs of HPS, such as shortness of breath and pulmonary edema, as well as a recent history of exposure to possibly infected rodents point to Hantaviruses as a differential diagnosis. The standard molecular-based test used for diagnostics is the reverse- transcriptase polymerase chain reaction (RT-PCR) test, which is able to detect presence of viral RNA in patient blood or serum samples [59,60]. Serological tests are also completed on patient serum to determine presence of anti-viral IgM and IgG antibodies [6,59,60]. The capture ELISA is the most widely used serological assay, able to detect IgM antibodies against the viral nucleocapsid (N) protein [6,59,60]. Detectable levels of IgM antibodies are present from the beginning of the prodrome phase, while IgG antibodies are typically detected in individuals during the intermediate and severe stages of disease [6,60].

There are currently no FDA approved vaccines or therapeutics for both HFRS and HPS, however the development of an effective vaccine is of high importance for HFRS due to the high number of cases present each year within Europe and Asia. A popular HFRS vaccine, Hantavax, has been administered to residents of high-risk areas in Korea since the

1990's [61–63]. This inactivated Hantaan virus-based vaccine presents no serious side effects and induces a powerful short term immune response, however its long-term effectiveness is poor with only half of individuals responding to boosters two years after the initial vaccine dose [64]. Several DNA-based vaccines are currently in the process of passing clinical trials. One of these is the HNTV/PUUV dual vaccine that targets the M segment of these viruses, proven to be effective within animal models and is currently in human clinical trials [63]. In contrast to the advancements of an HFRS vaccine, the selection of possible HPS vaccine candidates remains sparse due to the low number of cases. However, animal studies have proven that vaccination against the viral glycoprotein and/or nucleocapsid protein protects against lethal viral challenge within animal models [65–67]. These vaccine candidates have demonstrated success within animal models, but have yet to advance to clinical trials.

Ribavirin remains the most common antiviral administered to ANDV patients [63,68]. The mechanism of action involves disrupting the viral polymerase and introducing mutations within the viral genome, as Ribavirin is a nitrogen-base analog and becomes incorporated into the newly synthesized viral RNA strand [68]. Although studies have showed that ribavirin treatment provides protection within the lethal Syrian hamster model, these studies revealed that ribavirin is in fact only statistically beneficial when administered during the early course of disease [63,68,69]. Several human trials have been conducted with ribavirin as the treatment source and the final conclusions state that ribavirin does not decrease mortality and is ineffective when administered to patients who have progressed past the prodrome phase of disease [59,61,70]. Favipiravir is another antiviral that has

demonstrated protection against Hantavirus infections. Favipiravir demonstrated 100% protection against ANDV infection within the Syrian hamster model when administered up to three days post challenge [63,69]. However, as with ribavirin, Favipiravir provides no benefit when administered past the early course of disease [63,69]. Additional treatment options including lactoferrin, an iron-binding glycoprotein, and corticosteroids have been tested for HPS and HFRS, however lactoferrin proves to be effective if administered shortly post infection and treatment with corticosteroids demonstrates no significant benefit to HPS patients [61,63].

1.6.2 Passive Transfer Animal Studies

With vaccine research proving to be cost-ineffective and antiviral treatment demonstrating no statistical benefit to HPS patients, the current focus in the field of ANDV therapeutics is neutralizing antibodies. With HPS the common trend is that a reduced amount of neutralizing antibodies within an individual results in a more severe form of the disease, with average neutralizing titres of 1:3200 seen in mild cases and titres of 1:200 or less seen in severe cases [69,71]. Patients who do recover typically express a larger abundance of virus neutralizing antibodies [69]. For the past decade, multiple animal studies have evaluated the method of passive transfer using immune serum [67,72,73]. Vaccinations against the viral glycoprotein and nucleocapsid protein within hamsters resulted in the production of neutralizing antibodies that significantly protected animals against lethal challenge just 24 hours post immunization [66,67]. Passive transfer of immune rabbit serum targeting the nucleocapsid protein to Syrian hamsters resulted in complete protection against challenge when administered at day -1 and +5 post challenge [67]. In addition,

immune serum obtained from vaccinated Rhesus macaques provided full protection in the Syrian hamster model when administered up to 5 days post infection [67]. The success with animal-sourced neutralizing antibodies has opened the door to evaluating whether human or humanized neutralizing antibodies exhibit the same capabilities. Unsurprisingly, monoclonal neutralizing antibodies from human HPS survivors provide 100% protection against lethal challenge within the Syrian hamster model, and additionally humanized trans-chromosomal bovine IgG antibodies provide similar protection even when administered 5 days after challenge [74,75]. This demonstrated success provides evidence that neutralizing monoclonal and polyclonal antibodies can be an effective post-exposure treatment for HPS patients [69,74].

1.7 Human IgG Antibodies

Since their discovery almost 100 years ago, immunoglobulins continue to be of particular interest in regards to their pathogen-binding and cell activating properties [76]. Antibodies are abundantly present in human serum and can be divided into 5 classes based (**Figure 2**) on their physical structure and function: IgA, IgD, IgE, IgM, and IgG [76,77]. IgA is present as a dimer in high concentrations at mucosal surfaces, where its function is to neutralize invading bacterial and viral pathogens, preventing them from entering the human body through binding sites [76,78]. The function of IgD is not yet understood, however B cells can produce pathogen-specific IgD molecules which suggests they play a role in signalling pathways as IgD antibodies are often membrane-bound to B cells [76,78]. IgE is typically present at low concentrations within the body and plays an important role in sensitivity and allergic response [76,79]. IgE's bind receptors found on multiple types of effector cells such as mast cells and eosinophils, leading to induction of gene transcription

pathways and release of cytokines that stimulate inflammation [76,79]. IgG is the most abundant antibody found within the human body and plays critical roles in binding antigens, activating pathways, and directing multiple types of cells [76,79]. The production of IgG- specific antibodies occurs later in primary exposure and therefore plays a major role during secondary exposure, whereas an IgM response is seen during initial contact with a foreign pathogen or substance [76,79]. During primary infection, IgM-bound B-cells recognize foreign pathogens and secrete pentameric IgM structures, which in turn can recognize multiple antigens and stimulate destruction pathways [76,79].

There are four subclasses or isotypes of IgG in humans: IgG_1, IgG_2, IgG_3, and IgG_4 [77,80]. Each antibody is composed of two heavy chain subunits and two light chain subunits joined together by disulfide bonds (**Figure 2**) [77,80]. The two light chains, which can be lambda or kappa chains, are identical to one another and are 25 kDa in size, whereas the two identical heavy chains are of approximately double in size at 50 kDa each [77,80]. The light chains and heavy chains join to form the Fab fragment, fragment antigen binding, which consist of the V_H (variable heavy), CH_1 (constant heavy), V_L (variable light), and C_L (constant light) domains [77,80]. The CH_2 and CH_3 constant domains of both heavy chains make up the Fc fragment, and both Fc fragments are ultimately joined via disulfide bonds located within the hinge region [77,80]. The variable domains of the antibody are particularly important as the paratope(s) are responsible for recognizing and binding the epitope(s) of antigens [76,77]. Each individual variable domain is encoded by different V,D, and J gene segments that make up antigen-binding motifs termed ‘complementary determining regions’ [76,77].

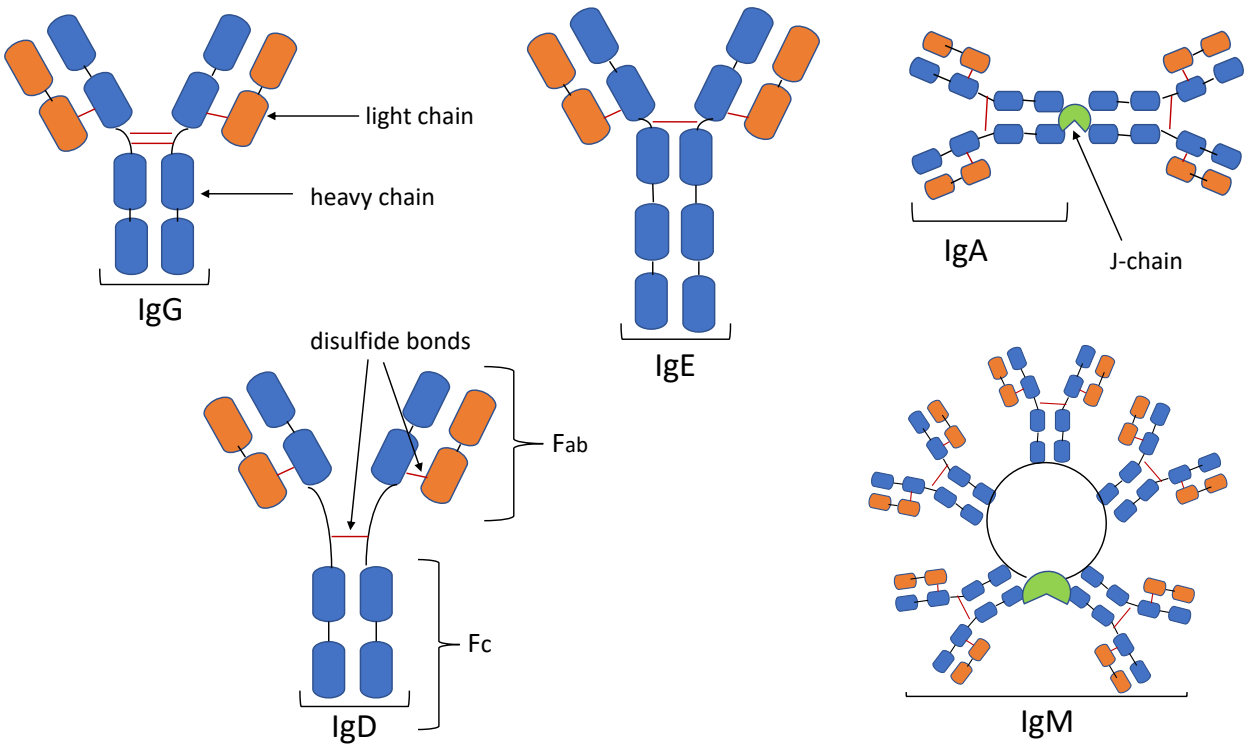

Figure 2. Structure of conventional human IgA, IgD, IgE, IgG, and IgM antibodies.

These genes undergo re-assortment to reveal a large repertoire of antibodies that have the potential of identifying multiple foreign pathogens, along with somatic hyper-mutation/ gene conversion which introduces mutations within the variable domain [76,77,81]. After several rounds of mutations and multiple sessions of re-assortment, B-cells producing antibodies with a high affinity to a particular antigen are selected for [76,77,81].

As mentioned above, IgG molecules play a critical role in antigen presentation and activation of pathways that lead to viral clearance [77,82]. During the acute phase of ANDV infection, IgM N-protein specific antibodies are predominately produced and IgG antibody production increases with progression to the secondary phase of infection [82]. Virus neutralizing IgG antibodies typically target the surface glycoproteins Gn and Gc, and individuals with high levels of neutralizing antibodies demonstrate a milder form of disease [82]. Neutralizing IgG antibodies are not only able to bind virus particles and prevent target cell entry, but are also able to bind Fc receptors via the Fc fragment and induce cell activation [77,80,83]. Activation of Fc receptors on macrophages results in destruction of large immune complexes and release of IFN-γ, activation of Fc receptors on B-cells results in the production of more virus-specific IgG antibodies, and activation of Fc receptors on granulocytes such as neutrophils result in phagocytosis of infected cells [80,84].

1.8 Alpaca IgG Antibodies

1.8.1 Structure and Function of Alpaca IgG Antibodies

The unexpected discovery of heavy-chain IgG antibodies in 1993 was the first example of naturally produced antibodies that differ from the conventional structure [85–87]. The

Camelidae mammalian family, which includes llamas, alpacas, and camels, naturally produce heavy-chain IgG antibodies that constitute anywhere from 10-50% of total IgG antibody in serum [87,88]. Heavy-chain antibodies are appropriately named as they do not possess any light chains nor contain CH_1 domains, which typically interact with the light chains in conventional antibodies (**Figure 3**) [85,88]. The genes for the CH_1 domain are actually present within the whole heavy-chain antibody sequence, however it is spliced during transcription and allows the variable domain to interact directly with the constant domain through a hinge region, resulting in a heavy chain that is approximately 45 kDa in size rather than the conventional 50 kDa size [88,89]. This structural difference is important for the secretion of heavy-chain antibodies, as conventional heavy chains remain within the endoplasmic reticulum until the heavy chain and light chains interact [86,88].

The main area of focus regarding heavy-chain antibodies is the variable domain, a small nanobody protein of 12-15 kDa in size (**Figure 3 b,c**) [86,88]. The variable domain (V_{HH}) is organized into conserved framework regions and variable complementarity determining regions (CDR's), with three CDR's placed between the four framework regions [85,86,88]. The region is folded into multiple β-sheets that are connected together, and the CDR loop structures contain antigen-binding paratopes [86,88]. An interesting finding is that the genes for both conventional heavy chains and heavy-chain only antibodies are located within the same locus of the *Camelidae* genome [88]. Sequencing analysis comparing the variable domain (V_{HH}) and conventional variable (V_H) regions reveals 80% homology, however there are several unique changes that attribute to the enhanced binding capabilities of these antibodies [85,86,88]. First, there are several hydrophobic to hydrophilic amino

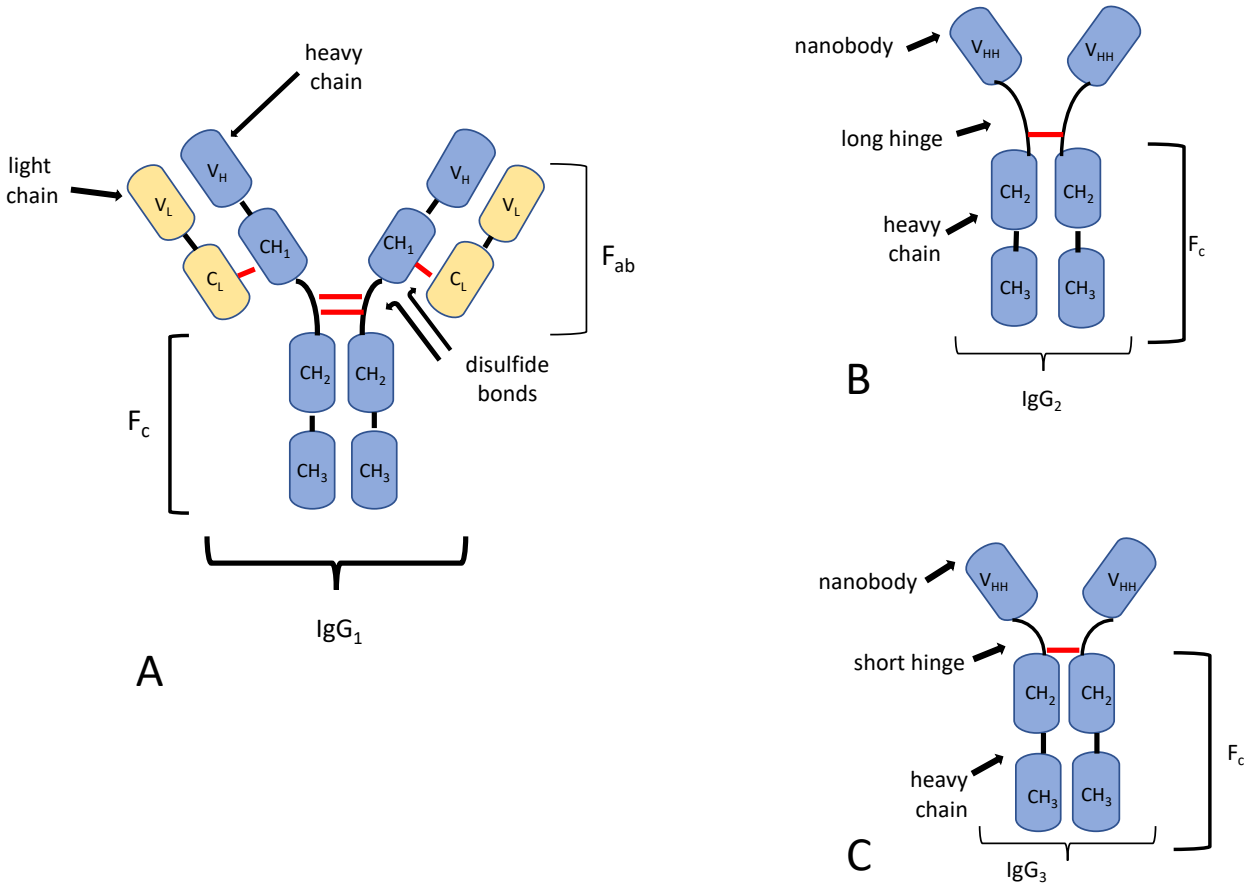

Figure 3. Structure of conventional IgG_1 alpaca antibody and IgG_2 and IgG_3 heavy-chain antibodies. Structure (A) corresponds to the conventional heavy-chain antibody, while (B) represents the long-hinge heavy-chain antibody and (C) represents the short-hinge heavy-chain antibody.

acid changes within framework region 2 that result in an increased solubility of these antibodies [85,86,88]. This adaptation is thought to have occurred as heavy-chain antibodies do not interact with light chains, meaning these changes would prevent unfavorable interactions between the hydrophobic antibody surface and hydrophilic blood plasma [85,86,88]. Second, the CDR1 and CDR3 loops of the heavy-chain V_{HH} are extended when compared to the V_H of conventional antibodies [85,87,88]. These extended regions have a unique convex shape and display a great amount of flexibility, stabilized by additional cysteine bonds within the loops, allowing the antibody to recognize unique epitopes that are typically inaccessible to conventional paratopes [85,87,88]. This adaptation is believed to have occurred due to the absence of a light chain which has additional antigen-binding regions [85,87,88].

Alpacas produce two types of heavy-chain antibodies, the long-hinged IgG_2 and the short-hinged IgG_3 (**Figure 3 b,c**), with heavy-chain antibodies accounting for roughly 50% of total IgG within the species [88,90]. The hinge region is comprised of repeats of glutamic acid (Glu) and proline (Pro), and the long hinge of IgG_2 is believed to be an adaptation to the splicing of the CH_1 domain [87,88]. Little is known regarding the exact function and production of heavy-chain IgG's compared to conventional IgG's in response to infection or vaccination strategies [91]. During initial infection, IgM antibodies undergo class switching where several antibody units are replaced and/or modified to yield IgG antibodies [91]. However, the class switching events that result in the production of heavy-chain IgG's is poorly understood. Normally, the modification of the IgM sequence particularly within the D-J elements allow for the proper amino acids to be incorporated

for the ultimate interaction between the heavy and light chains [91]. However, evidence strongly points to alpacas and other *Camelidae* members possessing unique B-cell mutation mechanisms that result in the exchange of amino acids, particularly from Tryptophan to Arginine, that prevent the association of heavy and light chains thereby resulting in the selection for heavy-chain antibodies [91]. Little is also known regarding the exact functions of each heavy chain antibody type, however studies have indicated that vaccination results in the production of effective neutralizing IgG_3 and IgG_1 antibodies, with IgG_1 levels slightly dominating as they are more abundantly produced [91]. The production of neutralizing IgG_2 however was seen in limited amounts, although all three IgG antibody types are effectively capable of binding Fc receptors on macrophages [91].

1.8.2 Current Advancements with Heavy-Chain Antibodies

Multiple efforts have been made to evaluate the potential of heavy-chain antibodies as diagnostic tools and/or treatments against foreign pathogens. The most successful viral nanobody developed to date is the ALX-0171 Respiratory Syncytial Virus (RSV) treatment, currently in Phase 2 clinical trials [92–94]. This trivalent nanobody has demonstrated a greater neutralizing capacity when compared to the currently used RSV monovalent antibody treatment, and possesses the unique qualities of being easily manufactured *in vitro* and delivered directly into the lungs through an inhaler/ nebulizer [92–94]. Additional nanobody treatments have been developed in the field for targeting the surface glycoproteins of Influenza Virus and Middle Eastern Respiratory Syndrome (MERS-CoV), both of which provided protection against lethal viral challenge in their appropriate animal models [95,96].

Using nanobodies as potential diagnostic tools has also been evaluated for several infectious viruses such as Dengue Virus (DENV), and for bacteria such as *Neisseria* [97,98]. For Dengue Virus, Fatima *et al.* explored the possibility of incorporating nanobodies into a quick and easy lateral flow test to identify viral antigen within samples [97]. The viral specific nanobody not only effectively bound viral antigen, it had a greater specificity when compared to its mouse monoclonal antibody counterpart [97]. When evaluating the use of nanobodies as bacterial detection agents, Wilken *et al.* developed a unique lipopolysaccharide receptor-targeting nanobody that effectively blocked interaction with its ligand [98]. Several additional nanobodies have been explored for targeting and detecting *Clostridium difficile*, *Streptococcus mutans*, and protozoa such as trypanosomes [98–100].

Nanobody treatments and diagnostic tools are still in early development, however they have enormous potential in the field due to their unique properties. Because of their elongated CDR regions, nanobodies can access certain epitopes that are difficult to detect with conventional monoclonal antibodies or antibody fragments [97,101]. In addition, the ability to link nanobodies together to create a dimer or trimer is attractive because it allows for the targeting of multiple epitopes [92,102]. Furthermore, the ability to deliver the nanobody treatment using a nebulizer allows for a quick and less invasive treatment approach [92].

1.9 Study Rationale, Hypothesis, and Objectives

Past protection studies within the Golden Syrian hamster model have successfully demonstrated that neutralizing IgG antibodies against lethal ANDV challenge, when administered early on, are capable of preventing the development of HPS/ HCPS [67,74,75]. The following thesis aims to investigate the level of protection that neutralizing IgG alpaca antibodies will have against lethal ANDV challenge. Alpaca IgG antibodies possess unique and attractive qualities, and neutralizing alpaca IgG antibodies have never been developed for ANDV. The unique properties of alpaca IgG's are a result of the unique V_{HH} domain structure, including increased solubility through amino acid changes, and the ability to bind typically inaccessible epitopes due to extended CDR loops [85,87,88]. To obtain neutralizing alpaca IgG antibodies, alpacas will be vaccinated with a DNA vaccine and adjuvant over a 12-week vaccination schedule to allow for the development of a potent neutralizing antibody response. Previous vaccination studies have successfully obtained sufficient levels of neutralizing antibodies from serum over a period of 9-12 weeks [90,103]. **The central hypothesis for this project is that DNA vaccination of alpacas against the ANDV glycoprotein will result in an immune response leading to the production of neutralizing IgG antibodies. Additionally, purified alpaca IgG antibody from vaccinated animals will provide protection against lethal ANDV challenge within the Golden Syrian hamster model.**

This hypothesis is addressed in the following objectives:

1. Develop and confirm the expression of ANDV glycoprotein using the pCAGGS DNA vaccine by traditional Western blot and tissue culture expression experiments. (Chapter 3.1)

2. Evaluate the ability of the pCAGGS-ANDVGPC vaccine to generate neutralizing antibody titres within 3 vaccinated alpacas at each serum collection time point. Neutralizing titers will be assessed using a plaque reduction neutralization test (PRNT's) with recombinant Vesicular Stomatitis Virus expressing ANDV glycoprotein (VSV-ANDVGPC) (Chapter 3.2).

3. Assess the ability of purified polyclonal alpaca IgG and the individual subtypes (IgG_1, IgG_2, and $IgG_{3)}$ to neutralize recombinant VSV-ANDVGPC (Chapter 3.3).

4. Evaluate the bioavailability of purified alpaca PcIgG within the Golden Syrian hamster model. Serum levels of PcIgG will be assessed at various time points up to a 7 days after a single administration of PcIgG (Chapter 3.4)

5. Evaluate the protection of a neutralizing alpaca PcIgG antibody treatment against lethal ANDV challenge within the Golden Syrian hamster model. This will be conducted by a proof of concept animal study, where animals will be challenged with a lethal dose of ANDV and treated post-exposure with the purified alpaca PcIgG treatment (Chapter 3.5)

Chapter 2. Material and Methods

2.1. Animal Cell Lines

Human Embryonic Kidney 293 T-cells (HEK 293T) were obtained from ATCC (Maryland, USA). These cells were used as a transfection host for the pCAGGS-ANDV GPC plasmid. African Green Monkey Kidney cells (VERO E6) were additionally obtained from ATCC (Maryland, USA). These cells were used for PRNT's (Plaque Reduction Neutralization Assays) to determine the titre of ANDV-neutralizing alpaca antibodies.

2.2 Methods

2.2.1 Vaccine Design and Preparation

The pCAGGS-ANDV-GPC vaccine used for these experiments was previously constructed in the laboratory [66]. In summary, the ANDV glycoprotein sequence (GenBank) was cloned into the multiple cloning site of pCAGGS at restriction cut sites KpnI and NheI. Following cloning, plasmids were transformed into Stellar E.coli cells and plated onto LB+ 100ug/mL ampicillin selective media. The insert was sequenced from the positive transformants using ANDV-specific primers and successful cloning was confirmed with PCR.

2.2.2 Preparation of Plasmid Vaccine

Production of pCAGGS-ANDV-GPC vaccine was based on bacterial culture. A glycerol stock of pCAGGS-ANDV-GPC in Stellar E.coli was used to streak LB Miller + 100 μg/mL Ampicillin agar plates (Appendix B). The plates were incubated overnight at 37^{o}C to promote bacterial growth. A single colony was used to inoculate 5mL of LB Miller + 100

μg/mL Ampicillin broth (Appendix B). The starter culture was incubated at 37°C for 8 hours at 250 rpm, and added afterwards to 2 liters of LB Miller + 100 μg/mL Ampicillin broth (Appendix B) for bacterial growth overnight. Bacterial cell pellets were obtained from the liquid culture through centrifugation. The Qiagen Plasmid Plus Giga kits (Qiagen, Toronto, ON, Canada) were used to isolate plasmid for subsequent experiments. The manufacturers protocol provided by Qiagen was followed. Purified plasmid was eluted in Ambion™ Nuclease-Free Water (Fisher Scientific, Ottawa, ON, Canada), and dsDNA concentration was measured using the Nanodrop™ One Microvolume UV-Vis Spectrophotometer (Fisher Scientific, Ottawa, ON, Canada). Plasmid was aliquoted and stored at -80°C.

2.2.3 Tissue Culture Transfection

Tissue culture plates (6-well) were seeded with 293T cells at 50% confluence in DMEM+5% FBS+ 1% Penicillin/Streptomycin. The following day, 70-80% confluent cells were transfected with a reaction mixture. 200ul of Opti-MEM enriched media was combined with 2ug of plasmid DNA in a 1.5mL Epindorf tube. The X-treme Gene HP transfection reagent was allowed to sit at room temperature for 15 minutes, after which 6ul was added to the transfection reaction. The mixture was vortexed and allowed to incubate at room temperature for 15 minutes. During incubation, cell media from the 6-well plate was replaced with fresh DMEM+5% FBS+ 1% Penicillin/Streptomycin. The reaction mixture was added drop-wise to the well with a pipette and the plate was rocked gently to distribute the reaction evenly over the cells. The plate was incubated at 37°C for 72 hours

and examined using the EVOS M5000 Imaging System at various time points. The mock transfection reaction was performed as described above but lacked added DNA.

2.2.4 Western Blot and LI-COR Imaging

Cells were harvested for Western blot analysis by removing culture supernatants and replacing it with 500uL of Protein Denaturing Buffer (Appendix B). Cell lysate was collected and placed directly into a QIAshredder spin column and centrifuged at max speed for 2 min to homogenize the lysate. Confirmation of ANDV glycoprotein expression was done via Western blot. In summary, a 20uL reaction was prepared using 4uL of cell lysate (10ug of ANDV-GPC protein, Bolt™ (4X) LDS Sample Buffer (Fisher Scientific, Ottawa, ON, Canada), and Ambion™ Nuclease-Free Water (Fisher Scientific, Ottawa, ON, Canada). Reaction was incubated at 95ºC for 10 minutes. Approximately 1.5uL of MagicMark™ XP Western Protein Standard (Fisher Scientific, Ottawa, ON, Canada) and 10uL of reaction were loaded onto a Bolt™ 4-12% Bis-Tris Plus gel (Fisher Scientific, Ottawa, ON, Canada) and ran at 140V. Protein transfer occurred using the iBlot®2 Dry Blotting System (Fisher Scientific, Ottawa, ON, Canada). The nitrocellulose membrane was incubated with Western Blot Blocking Reagent (Appendix B) for 1 hour at room temperature. Afterwards, Blocking Reagent was replaced with 10mL of Western Blot Antibody Diluent (Appendix B) with a 1:5000 dilution of either Mouse Monoclonal Anti-Glycoprotein C of Andes Virus IgG fraction (AMSBIO LLC, Cambridge, MA, USA) (Appendix A) or Mouse Monoclonal Anti-Glycoprotein N of Andes Virus IgG fraction (AMSBIO LLC, Cambridge, MA, USA) (Appendix A) and incubated overnight. The membrane was washed with Western Blot Wash Buffer (Appendix B) and incubated with

10mL of Western Blot Antibody Diluent (Appendix B) with a 1:5000 dilution of IRDye 800CW Goat anti-Mouse IgM (0.5mg) (Cedarlane, Burlington, ON, Canada). Membrane was washed a final time and imaged using the Li-Cor® Odyssey Imaging System (LI-COR Inc., Lincoln, NE, USA).

2.2.5 Ethics

Alpaca's (Vicugna pacos) used for the vaccination experiment were housed at VIDO-InterVac (Vaccine and Infectious Disease Organization) under conditions approved by the University of Saskatchewan Animal Care Committee (ACC). Three alpaca's of roughly 80 kg were purchased from local farms and housed in a CL2 facility for at least 7 days prior to the start of vaccination. Animals received food, water, and enrichment material during the duration of the experiment. During the acclimatization period, animals were trained to wear ropes and halters in order to prepare for blood collections and vaccinations. Blood collections were performed prior to each vaccination and plasma was isolated and used for downstream in-vitro and in-vivo studies. Animals were monitored daily during the course of the experiment, and were humanely euthanized at the end of the experiment under approved ACC regulations. All manipulations were conducted and monitored by trained veterinary staff at VIDO-InterVac.

Syrian Hamster experiments were performed at the Canadian Science Centre for Human and Animal Health at the National Microbiology (NML) facility of Public Health Agency of Canada. All animal experiments were approved by the Animal Care Committee (ACC) under the Canadian Council on Animal Care guidelines and regulations. Female hamsters

were used for both experiments as this model has been extensively characterized in females. All animals were purchased from Charles River Laboratories and housed for at least one week prior to start of experiments in the animal holding facility to acclimatize to the environment. Animals were housed in appropriate cages, provided with free access to food and water, and were monitored daily during the course of the experiments.

2.2.6 Alpaca Vaccination Schedule

The following vaccine design was approved and conducted by animal services at VIDO-InterVac in Saskatoon, Saskatchewan. Three outbred male alpacas weighing approximately 80kg each were purchased from rural sources and housed in the biosafety level 1 animal facility at VIDO-InterVac for a minimum of 1 week for acclimatization. Each animal received 2x 0.5 mg of vaccine (pCAGGS-ANDV GPC plasmid) and 160uL of Invivo-Jet PEI Transfection reagent (Appendix A) intradermaly, with the vaccine delivered into both hind legs. Each animal initially received a total of 4 vaccinations, each administered after a 3-week interval for a total of 4mg of vaccine over the 12 week course. Prior to each vaccination, 10mL of blood was collected from each animal and plasma was obtained to determine neutralizing antibody levels. At day 66 (9^{th} week), 100mL of blood was collected for PBMC isolation. Following a break, animals were boosted twice at days 228 and 249, with animal 3 receiving boosts intramuscularly. A large blood collection occurred at day 270 to isolate plasma for animal studies, isolated by placing blood with Ficoll-Paque media into sterile centrifuge tubes. Samples were spun to allow for a gradient to occur. The top layer of plasma was carefully pipetted and collected from the tube, while the PBMC's were carefully pipetted from the interface. Animals were housed at VIDO-

InterVac during the duration of the experiment. Animals were euthanized according to Animal Use Protocol methods approved at VIDO-InterVac.

2.2.7 Plaque Reduction Neutralization Test (PRNT)

Plasma collected from all animals was heat-inactivated at 56ºC for 30 min. PRNT assays were conducted with either heat inactivated plasma, purified polyclonal IgG, or IgG subtypes. Twelve-well cell-culture plates were seeded with Vero E6 cells the night prior and were incubated overnight at 37ºC to reach 100% confluence. Alpaca plasma or purified IgG was diluted in HyClone™ Dulbecco's Modified Eagles Medium (Fisher Scientific, Ottawa, ON, Canada) in a 2ml dilution block (include reference) starting at a dilution of 1:20 to 1:20,480. VSV-ANDV was prepared to a 50 pfu/ml concentration and added 1:1 to the diluted plasma. The plasma / antibody and virus mixture was incubated at 37ºC for 1 hour, after which 250uL of each mixture was placed on a 12-well cell culture plate in triplicate wells. Virus inoculum and cells were incubated at 37ºC for 1 hour. Virus inoculum was removed from cells and 1ml of overlay (2% low melting point agarose) was added to each well. After 3 days of incubation, the overlay was stained with crystal violet overnight. The following day the crystal violet and agarose was removed from each well and plaques were counted. To calculate the % neutralization values for the alpaca plasma collections as well as for PcIgG, the number of plaques in each well were subtracted from the average number of plaques in the control wells inoculated with 50 pfu/ml of VSV-ANDV. The % neutralization values were then averaged per dilution. The same method was used to determine the % neutralization for the IgG subtype analysis of the day 63, 66,

and 84 collection, however values from each well were plotted to yield an average and margin of error.

2.2.8 Purification of Alpaca PcIgG and IgG Subtype Antibodies

HiTrap HP A and G columns (1ml and 5ml) (GE Healthcare, Mississauga, ON, Canada) were equilibrated with HiTrap Protein A and G Column Binding Buffer (Appendix B). Alpaca plasma prepared as stated in 2.2.7 was applied to the HiTrap HP G column first at a rate of 0.5ml/min. Column was washed with HiTrap Protein A and G Column Binding Buffer (Appendix B), and alpaca IgG_3 antibody was eluted using Alpaca IgG_3 Elution Buffer (Appendix B). Following IgG_3 elution, alpaca IgG_1 was eluted using Alpaca IgG_1 Elution Buffer (Appendix B). Flow-through was collected and applied to the HiTrap Protein A column to isolate IgG_2 using the Alpaca IgG_2 Elution Buffer (Appendix B). To isolate polyclonal IgG (PcIgG), plasma was directly applied to a HiTrap Protein A column (GE Healthcare, Mississauga, ON, Canada) and PcIgG was eluted using the Alpaca Polyclonal IgG Elution Buffer (Appendix B).

2.2.9 Dialysis and Concentration of PcIgG and Subtype Antibodies

Eluted antibodies were preserved by adding 10% of Antibody Stabilizing Buffer (Appendix B), and were concentrated using the Pierce™ Protein Concentrator PES 10K MWCO (2-6 ml, 5-20ml) (Fisher Scientific, Ottawa, ON, Canada) (Appendix A). Antibodies were dialyzed in Gibco™ Phosphate Buffered Saline pH 7.2 (1X) (Fisher Scientific, Ottawa, ON, Canada) (Appendix A) and IgG concentrations were measured using the proteinA280

setting of the Nanodrop™ One Microvolume UV-Vis Spectrophotometer (Fisher Scientific, Ottawa, ON, Canada) (Appendix A).

2.2.10 Protein Gel Electrophoresis and Staining

Approximately 10ug of purified IgG_1, 10ug of IgG_3, and 5ug of IgG_2 from alpaca animal 1 day 0 was loaded onto a Bolt 4-12% Bis-Tris gel (Fisher Scientific, Ottawa, ON, Canada) to confirm correct isolation of IgG alpaca subtypes using the AKTA Pure FPLC chromatography system. The Magic Mark XP Protein Standard ladder (Fisher Scientific, Ottawa, ON, Canada) was used to determine band sizes. Each well contained 1X Bolt™ (4X) LDS Sample Buffer (Fisher Scientific, Ottawa, ON, Canada), and Ambion™ Nuclease-Free Water (Fisher Scientific, Ottawa, ON, Canada). Reaction was incubated at 95^0C for 10 minutes prior to loading onto gel. Gel was run at 120 V for 40 min, and rinsed 3 times with 100ml deionized water for 5 minutes each. Gel was incubated in SimplyBlue™ Safestain (Fisher Scientific, Ottawa, ON, Canada) for 1 hour at room temperature while shaking at 200 rpm, and washed for 1 hour with deionized water. Gel was imaged using the Li-Cor® Odyssey Imaging System (LI-COR Inc., Lincoln, NE, USA).

2.2.11 Pharmacokinetic Study Design

A pharmacokinetic study was conducted using alpaca PcIgG to determine the half-life of alpaca IgG antibodies in the Syrian hamster model. Plasma from animal 1 was purified using the FPLC AKTA Pure system to obtain PcIgG, as stated in section 2.2.8. Antibodies were dialyzed, concentrated (section 2.2.9), and the final preparation was filter sterilized

using a 0.22um syringe filter. Four Golden Syrian hamsters were purchased from Charles River laboratories at 4-6 weeks of age and acclimatized in the CL2 Veterinary Technical Services facility at the National Microbiology Laboratory in Winnipeg, Manitoba for 1 week prior to the commencement of the study. A pre-bleed was collected from each hamster 7 days prior to the experiment via the jugular vein using a 20G 1 inch needle. Each animal received 100 mg/kg of purified alpaca PcIgG subcutaneously (20G 1 inch needle) and serum from each animal was collected at the following time points: 6, 24, 48, 72, 96, 120, 144, and 168 hours post treatment. Animals were euthanized after the experiment was completed according to Canadian Council on Animal Care regulations.

2.2.12 Alpaca PcIgG Antibody Detection by ELISA

Serum was isolated from hamster blood collection time points as listed in section 3.5.1. A standard curve was created using an identical alpaca PcIgG sample as administered to each hamster in the pharmacokinetic study. For the standard curve, wells of a Costar 96-well flat bottom plate (Corning, USA) were coated with PBS and a mixture of 1ul of pre-bleed hamster serum (collected from hamsters 1 week prior to the experiment) plus alpaca PcIgG at 44.4 mg/ml starting from a 1/10000 dilution to a 1/ 2.48 x 10^7 dilution. Hamster serum samples were diluted 1/100 with PBS for an ELISA. The plate was coated overnight at 4^0C. Wells were then washed 4 times with 150µL of PBS 0.1% Tween 20, and blocked overnight with 5% skim milk powder in PBS (VWR, Mississauga, ON, Canada). Wells were washed 4 times with 150µL of PBS 0.1% Tween 20 and Goat anti-llama IgG (H+L) HRP-conjugated secondary antibody (Fisher Scientific, Ottawa, ON, Canada) was added to each well at a 1/5000 dilution. The plate was left at room temperature for 60 min and

then washed 4 times with 150µL of PBS 0.1% Tween 20. After the wash, 50µL of ABTS A/B Peroxidase Substrate reagent mix (VWR, Mississauga, ON, Canada) was added to each well. The plate was incubated for 30min in the dark and absorbance was measured at 405nm using the Synergy HTX Multi-Mode Reader (Biotek, VT, USA). Hamster serum samples were run in duplicate for the Elisa.

2.2.13 Alpaca PcIgG Protection Study Design

The following protection study was completed under the approved Animal Use Document (AUD) regulations and CCAC regulations. Twenty-seven Golden Syrian hamsters at 4-6 weeks were purchased from Charles River Laboratories and transported to the CL2 Veterinary Technical Services facility at the National Microbiology Laboratory in Winnipeg, Manitoba. Animals were acclimatized in the CL4 facility for 1 week prior to the start of the experiment. Animals were separated into 3 groups of 9 each, one group serving as the negative treatment control (receiving PBS), one group receiving naïve PcIgG treatment (purified from animal day 0 collection), and one group receiving the high neutralizing titre PcIgG treatment purified from animal 1 at day 270 (serum $PRNT_{80}$ of 1/640). The PcIgG treatments were isolated and prepared as described in sections 3.3 and 3.4. Each animal received 150 focus forming units of *Andes virus* via the intraperitoneal route using a 20G needle (1 inch). At days +1 and +3 post infection, each animal received 400ul of treatment subcutaneously using a 20G needle (1 inch). At 6 days post-challenge, 3 hamsters from each group (total of 9 animals) were euthanized to assess viral load. Blood and tissues from liver, lung, heart, and kidney were harvested upon euthanasia and stored under standard CL4 protocol. The experiment ended after 28 days post-challenge, and

survivors were euthanized following approved Animal Use Document procedures and Canadian Council on Animal Care (CCAC) regulations.

2.2.14 Viral RNA Detection in Tissues using qRT-PCR

Tissue samples harvested from day 6 hamsters (section 3.6.2) were collected and homogenized in 600µL RLT lysis buffer (Qiagen, Hilden, Germany), centrifuged, and aliquoted. RNA was extracted using the RNeasy mini kit (Qiagen, Hilden, Germany) from tissue samples, and RNA was extracted from blood collections using the Viral RNA mini kit (Qiagen, Hilden, Germany). To detect levels of ANDV S segment RNA, RT-qPCR was performed using a QuantStudio3 and ANDV-specific primers and probes (**Table 1**). RT-qPCR run consisted of reverse transcription to cDNA at 50^0C (30 min), Taq activation at 95^0C (15 min), and 40 cycles of amplification at 94^0C for 15 s followed by 60^0C for 60 s. Samples were compared against a standard curve of ANDV S segment in vitro transcribed RNA starting from 5 x 10^7 S segment copies and diluting to 5 copies.

Table 1. ANDV-specific primer and probe sequences used for RT-qPCR. RT-qPCR was performed on extracted RNA from collected animal tissues the QuantStudio3 system (section 3.6.3).

Material	**Sequence**
ANDV Probe	FAM-ACGGGCAGCTGTGTCTACATTGGA-TAMRA
ANDV Forward Primer	5’ AAGGCAGTGGAGGTGGAC
ANDV Reverse Primer	5’ CCCTGTTGGATCAACTGGTT

2.2.15 Statistical Analysis

GraphPad Prism 5 software was used to graph and analyze data from above mentioned studies. To depict the % neutralization values for each alpaca plasma time point, the average of the triplicate wells (as mentioned in section 2.2.7) were plotted using a standard X and Y grouped plot, with blood collection time points as X values and % neutralization values as Y values. For the PcIgG PRNT analysis, the PcIgG concentration (dilutions of 1:4) was designated as X values and were transformed using X= log (X). Transformed values were analyzed using a nonlinear regression (curve fit) and values were plotted to follow a log (agonist) vs. normalized response variable slope. The approximate Ec50 values, which corresponds to the concentration of the antibody at which we see 50% of the maximum neutralization response, were extrapolated from the nonlinear fit analysis. For the alpaca IgG subtype analysis, % neutralization values were calculated for each well. Results were plotted as mentioned above for the PcIgG PRNT's.

To determine the presence of alpaca PcIgG within the blood stream of Golden Syrian hamsters at different time points (section 2.2.11 and 2.2.12) using an ELISA, the x values (measured OD values) were transformed using X= log (X), and PcIgG concentration values were determined by interpolating X mean values using the standard curve. The extrapolated mean PcIgG concentration was plotted on the Y axis and time points plotted on the X axis. For the survival analysis of infected vs treated animals, a log rank Mantel-Cox test was used with a p value cut off of 0.05. For the comparison of viral genome copies in the various tissues between the treated and control groups, a Two-way Anova with correction for multiple comparison using a Tukey's test was conducted.

Chapter 3. Results

3.1 Development of pCAGGS-ANDV-GPC Vaccine

3.1.1 Rationale

The pCAGGS-ANDV-GPC vaccine used for these experiments was previously constructed at the National Microbiology Laboratory (Materials & Methods 2.2.1) [104]. Typically, DNA vaccination experiments have been conducted in a multitude of animals, as well as humans, having been made using the pVAX vector with a CMV promoter [105,106]. The vector pVAX is commonly used for expression as the simple vector construction typically allows for easy cloning and selection [107]. However, cloning of ANDV-GPC into the pVAX vector proved to be incompatible so we chose an alternative plasmid using the beta-actin promoter (pCAGGS). Possible reasons for the unsuccessful pVAX-ANDV-GPC include incorrect insertion of the sequence within the plasmid. Correct sequence orientation is important for cloning, especially as pVAX requires a start codon and specific initiation sequence for translation to occur [108–110]. Additionally, an incompatible host system would cause a lack of protein expression. Thus, the preparation and confirmation of ANDV glycoprotein expression in tissue culture was essential before conducting vaccination experiments. We hypothesized that cells transfected with pCAGGS-ANDV-GPC would fully express both G_n (GP_1) and G_c (GP_2) ANDV glycoproteins. The following objective was established to test the feasability of the pCAGGS vector for vaccination in alpacas.

3.1.2 Objective

Develop and confirm the expression of ANDV glycoprotein using the pCAGGS DNA vaccine by traditional Western blot and tissue culture expression experiments.

3.1.3 Results

The pCAGGS-ANDV-GPC plasmid and a positive control plasmid (pCAGGS-GFP) were grown in *E.coli* and purified using the methods outlined in section 2.2.2 and 2.2.3. Human Embryonic Kidney 293 T cells (HEK 293T) were seeded in a 6-well cell culture plate 1 day prior to transfection. Wells were either transfected (Materials & Methods 2.2.3) with pCAGGS-GFP, were mock-infected (transfection reagent only), or with pCAGGS-ANDV-GPC and images were captured at 24, 48, and 72 hours post-transfection (Figure 4). Expression of GFP was detectable at 24 hours and steadily increased up to 72 hours post-transfection indicating successful transfection conditions (Figure 4A). After 72 hours, cells from the pCAGGS-ANDV-GPC (Figure 4C) transfected wells were harvested and processed for Western Blot analysis (Materials & Methods 2.2.4) to confirm the expression of ANDV G_n (Figure 4A) and G_c (Figure 4B). Expression of G_n was confirmed to be 71 kDa (Figure 5A), while G_c was confirmed to be approximately 55 kDa (Figure 5B). Given the expression of both glycoproteins for each individual pCAGGS-ANDV-GPC plasmid preparation, each lot was used for subsequent alpaca vaccination experiments.

3.1.4 Summary

We successfully prepared pCAGGS-ANDV-GPC plasmid for vaccination and confirmed the expression of ANDV glycoprotein. The pCAGGS-ANDV-GPC plasmid will

subsequently be used in vaccination experiments to generate ANDV-specific neutralizing antibodies in alpaca's.

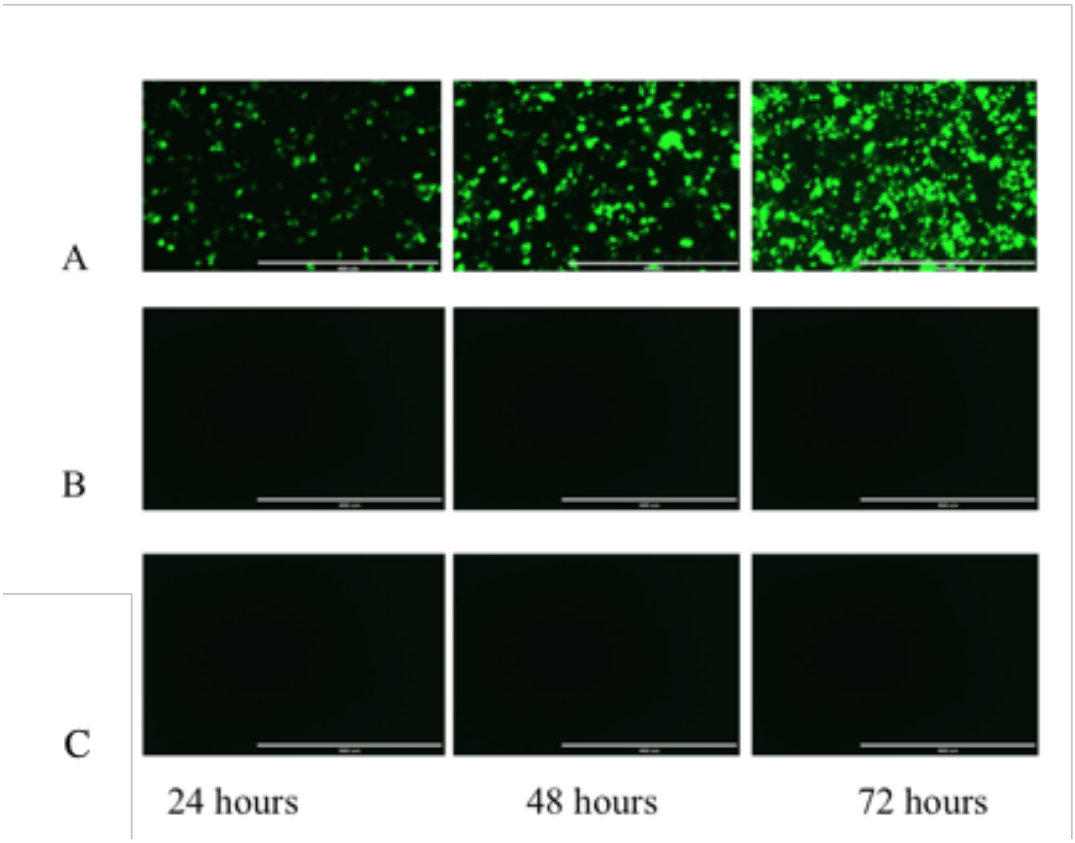

Figure 4. Transfection of pCAGGS-ANDV-GPC DNA Vaccine. Green fluorescent protein expression of pCAGGS-GFP at hours 24, 48, and 72 post transfection. Human Embryonic Kidney 293 T cells (HEK 293T) were seeded in a 6-well cell culture plate 1 day prior to transfection. Wells were either transfected with (A) 2 ug of pCAGGS-GFP, (B) mock-infected, or (C) 2 ug of pCAGGS-ANDV-GPC.

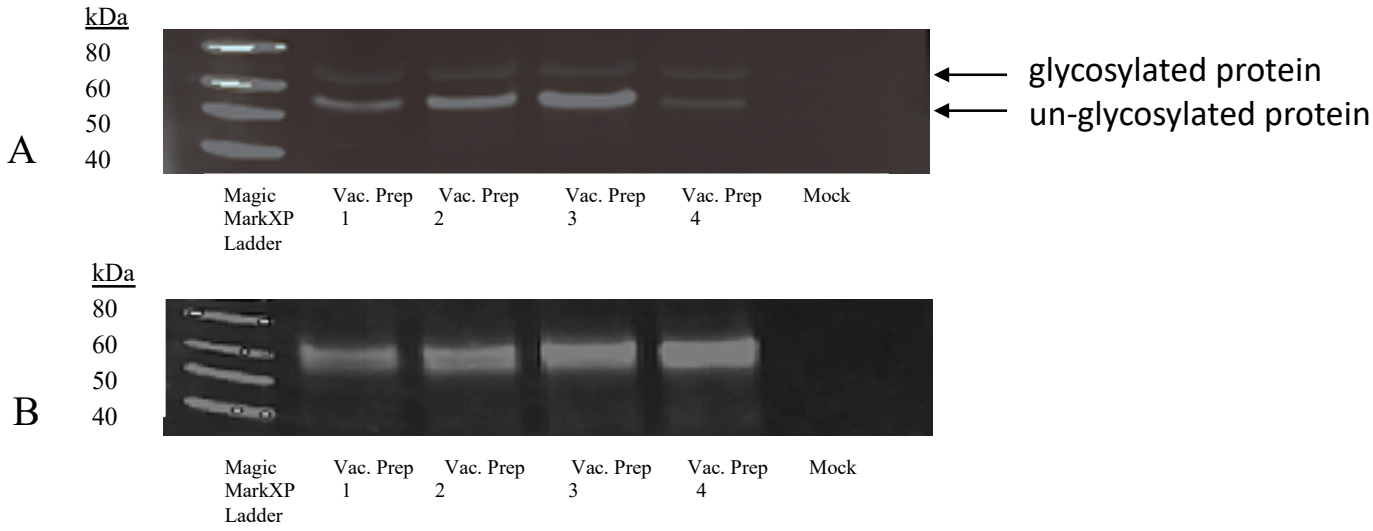

Figure 5. Confirmation of ANDV-GPC expression in HEK293T Cells. Western blot analysis of ANDV G_n (A) and G_c (B) protein expression from each individual vaccine preparation at 72 hours post-transfection.

3.2 Vaccination & Determination of alpaca neutralization titers

3.2.1 Rationale

Previous studies have indicated that alpaca/llama vaccination results in the successful production of neutralizing antibodies [90,95,111]. Vaccine studies using a DNA vector containing the ANDV-GPC sequence were capable of producing highly specific neutralizing IgG antibodies within animals, which in turn can be passively transferred to infected Syrian Golden hamsters as a treatment source [73–75]. Based on the success of these studies we proposed to explore the use of ANDV-GPC neutralizing antibodies sourced from alpacas as a form of treatment. As mentioned in section 1.8, alpacas produce unique IgG heavy-chain antibodies that possess many unique features [85,87,88]. These antibodies are able to neutralize viruses, and have been explored and developed for a wide range of pathogens [112–114]. Several studies have demonstrated the successful method of generating high titre neutralizing antibodies within alpacas and llamas [90,111,115]. Thus, we hypothesize that the vaccination of alpacas would result in the efficient production of anti-ANDV-GPC neutralizing IgG antibodies, that would eventually be evaluated in a lethal challenge experiment upon collection and purification.

3.2.2 Objective

Evaluate the ability of the pCAGGS-ANDV-GPC vaccine to generate neutralizing antibody titres within 3 vaccinated alpacas at each serum collection time point.

3.2.3 Results

Three alpacas were housed for the duration of the vaccination experiments at VIDO-INTERVAC following internal animal use guidelines outlined in section 2.2.5. Alpacas were vaccinated with pCAGGS-ANDV-GPC as specified in section 2.2.6 and plasma was collected from each animal at days 0, 21, 41, 63, 66, and 84, with vaccinations occurring at days 0, 21, 41, and 63 prior to each bleed. Animals were subsequently allowed to rest for several months, after which a second round of vaccinations was conducted at days 228, and 249 to assess whether neutralizing antibody production could be improved. All plasma collected was analyzed using a VSV-ANDV PRNT assay outlined in section 2.2.7. Animal #1 had the earliest and highest response to the vaccinations (**Figure 6**). The $PRNT_{80}$ titers increased with animal 1, starting from 1/80 at day 41 to 1/1280 at day 63, to 1/2560 at day 66 and 84. After the rest, a reduction in neutralizing antibody titre of approximately 50% was observed for animal 1 at day 228. Following a boost on day 228, the neutralizing antibody titre rebounded to 1/2560. However, the two subsequent boosts did not improve the neutralizing antibody titre and decreased to 1/640 by day 270. Animals 2 and 3 responded poorly to the vaccination schedule and only reached $PRNT_{80}$ titers of 1/160 at days 66 and 84. Animal 3 continued to respond poorly despite switching to intramuscular administration for the day 228, 249, and 270 boosts. Surprisingly, the neutralizing antibody titre improved for animal 2 for day 228, increasing dramatically to 1/2560 at day 249 following a boost. However, the neutralizing antibody titre dropped to 1/320 at day 270 following the second boost. Immune hamster serum from a previous study was used as a positive control for all PRNT's conducted.

3.2.4 Summary

After several months of vaccinations, high titre neutralizing antibodies were successfully produced in animal 1. Plasma was isolated from each time point to assess neutralizing titres, and a large bleed at day 270 was purified and used in subsequent bioavailability and efficacy studies within the Golden Syrian hamster model.

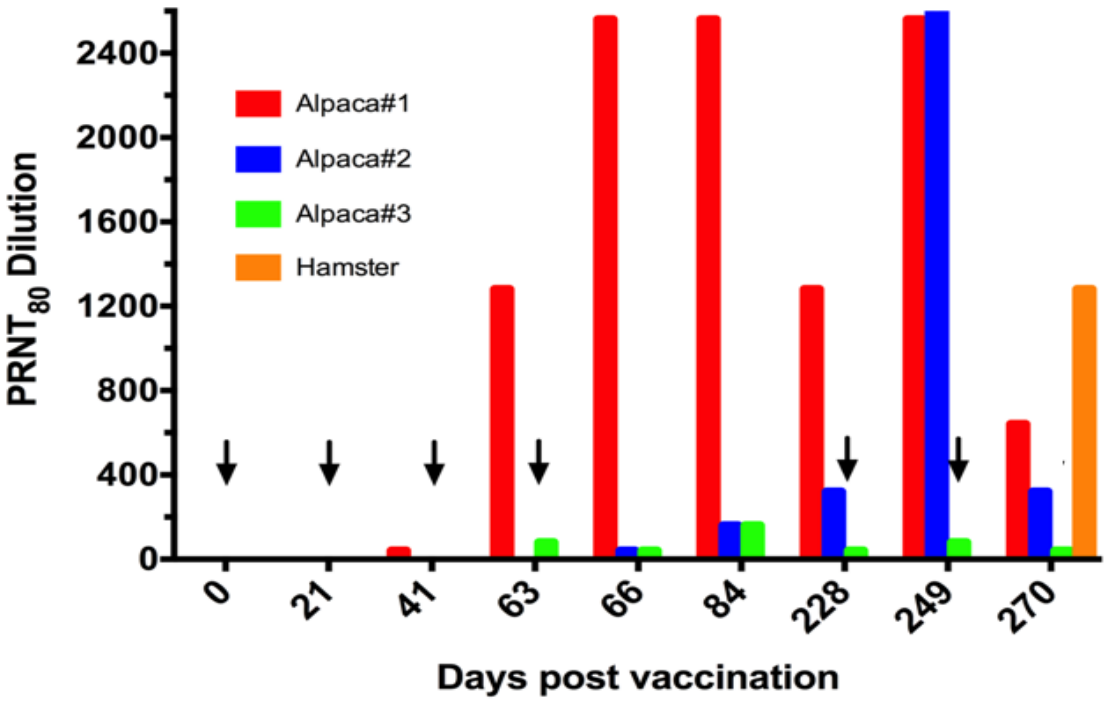

Figure 6 (A). Neutralizing alpaca antibodies following pCAGGS-ANDV-GPC vaccination. (A) $PRNT_{80}$ titers were calculated on all plasma collections from animals 1,2,3 using Vero E6 cells infected with VSV-ANDV. Immune hamster serum from a previous study involving VSV-ANDV vaccinations was used as a positive control. Arrows indicate vaccination points.

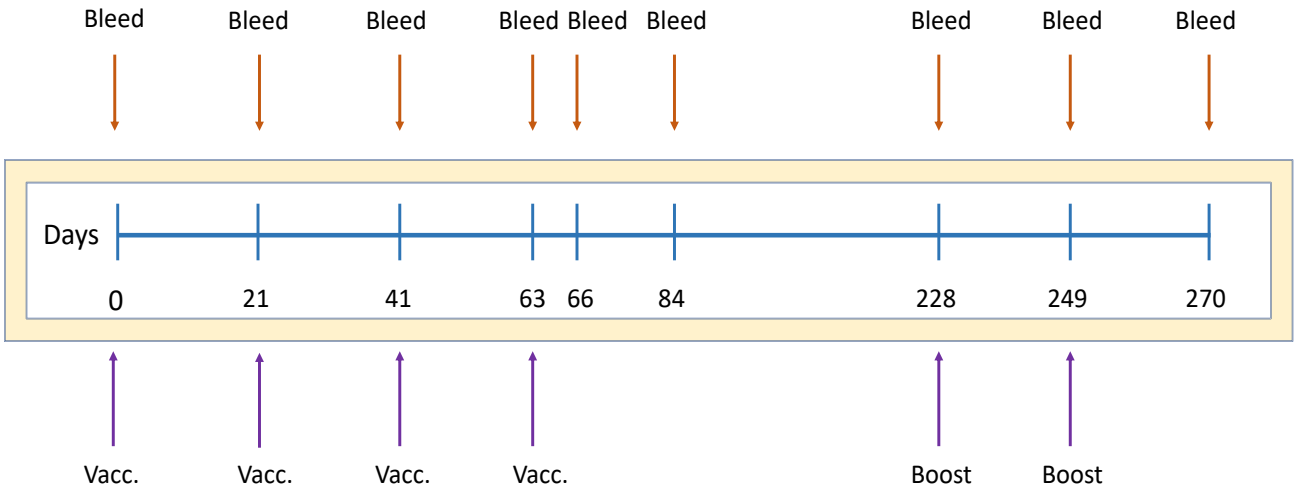

Figure 6 (B). Timeline of alpaca blood collections and vaccinations/boosts.

3.3 Analysis of polyclonal alpaca IgG and individual subtypes from alpacas

3.3.1 Rationale

Alpacas, along with additional members of the *Camelidae* family, produce conventional IgG_1 antibodies as well as IgG_2 (long hinge) and IgG_3 (short hinge) heavy- chain antibodies [87,89,90]. Purification of plasma to yield PcIgG is possible with liquid chromatography, as all alpaca IgG antibodies bind to protein A and thus can be isolated using a protein A column [90,103,116]. In addition, isolation of individual IgG subtypes is possible as IgG_1 and IgG_3 bind to protein A and protein G, while IgG_2 only binds to protein A [90,103,116]. Protein A and protein G, isolated from bacteria, are commonly used in the preparation of purification columns and can therefore be used for antibody isolation as they bind to the F_c domain [110]. Several studies have investigated the neutralizing properties of each individual IgG subtypes in alpacas, having confirmed that there are variations in neutralization levels between them [90,91]. We hypothesize that IgG subtypes will have different neutralizing capabilities against ANDV.

3.3.2 Objective

Assess the ability of purified polyclonal alpaca IgG and the individual subtypes (IgG_1, IgG_2, and $IgG_{3)}$ to neutralize recombinant VSV-ANDV-GPC.

3.3.3 Results

To investigate whether neutralization levels would vary between subtypes for this study, PRNT assays were conducted for each subtype separately, as well as for purified PcIgG. Alpaca 1 PcIgG was successfully isolated from alpaca 1 plasma at various timepoints using method 2.2.8. PcIgG bound to a protein A column, and was eluted after 20 column volumes

of a low pH buffer was applied through the column to disrupt the antibody Fc-protein A interaction (point B of Figure 7). The flow through (point A of Figure 7) consisted of various unbound plasma proteins such as albumin. The method described in 2.2.8 was also used to isolate individual alpaca IgG subtypes. Using a protein G column, alpaca IgG_1 and IgG_3 were successfully isolated as seen in Figure 8 (points B and C), through the use of buffers differing in pH. The flow-through collected in Figure 8 was kept and applied to a protein A column for the subsequent isolation of alpaca IgG_2 (Figure 9 B), as IgG_2 has a high binding affinity to protein A but not protein G. The individual subtypes were then visually analyzed using gel electrophoresis to confirm the purity and presence of the individual subtypes. The following bands are seen in Figure 11: a heavy chain band of ~45 kDa for IgG_3, a heavy chain band of ~45 kDa for IgG_2, and both a ~50 kDa heavy chain band and a ~25 kDa light chain band for the conventional IgG_1 antibody.

To identify neutralizing antibody activity of PcIgG, plasma from animal 1 at each time point was purified (method 2.2.8) and used in PRNT assays (method 2.2.7) as this animal responded the best to the vaccinations as seen in Figure 6. As expected no neutralizing antibody activity was seen for the day 0 collection (pre-bleed). The first two vaccinations, administered at day 0 and day 21, generated low levels of neutralizing PcIgG between 0 and 20%. After the 3rd vaccination on day 41, a large response was generated which was seen for the day 63 collection. For day 63, a neutralizing EC_{50} (dose of antibody at 50% of maximum neutralization activity) value of 3.35 ug/ml was observed (Table 2). The final vaccination at day 63 boosted the neutralizing antibody production once more within the animal, as the EC_{50} value for the day 66 collection decreased to 2.73 ug/ml. The EC_{50} value

dropped three weeks after the final vaccine dose prior to resting the animals on day 84 to 3.19 ug/ml.

To identify changes in neutralizing activity between alpaca IgG subtypes, plasma at days 63, 66, and 84 was purified from animal 1 (Figure 12,13,14). The response seen for the day 63 collection shows low EC_{50} values for IgG_3 (2.14 ug/ml) and IgG_1 (3.67 ug/ml) and a high EC_{50} value for IgG_2 (12.08 ug/ml) (Table 2). The EC_{50} value decreased for IgG_3 at day 66 (0.83 ug/ml) but increased for IgG_1 and IgG_2. This time point is after the animal received the 4^{th} vaccination, at day 63. The EC_{50} value increased for both IgG_1 and IgG_3 at day 84, however values for IgG_2 were not collected due to insufficient concentration after purification.

3.3.4 Summary

Alpaca PcIgG and subtypes IgG_1, IgG_2, and IgG_3 were successfully isolated using FPLC. The purity and size of the individual subtypes was also confirmed by protein gel electrophoresis prior to conducting neutralization experiments. Determination of neutralization activity in purified PcIgG revealed a dramatic increase in neutralizing IgG antibody titre after the 3^{rd} vaccine dose, as seen for the day 63 collection point. The EC_{50} value dropped slightly after the 4^{th} vaccine dose (day 66 collection), as was expected, and increased approximately 3 weeks later (day 84 collection). Determination of neutralization activity for individual alpaca IgG subtypes reveal high EC_{50} values for IgG_2 at days 63, 66, and 84. Values for IgG_1 and IgG_3 remain low for all 3 time points. Interestingly, the subtype

with the lowest EC_{50} value (the highest neutralizing capacity) was IgG_3, a heavy-chain antibody

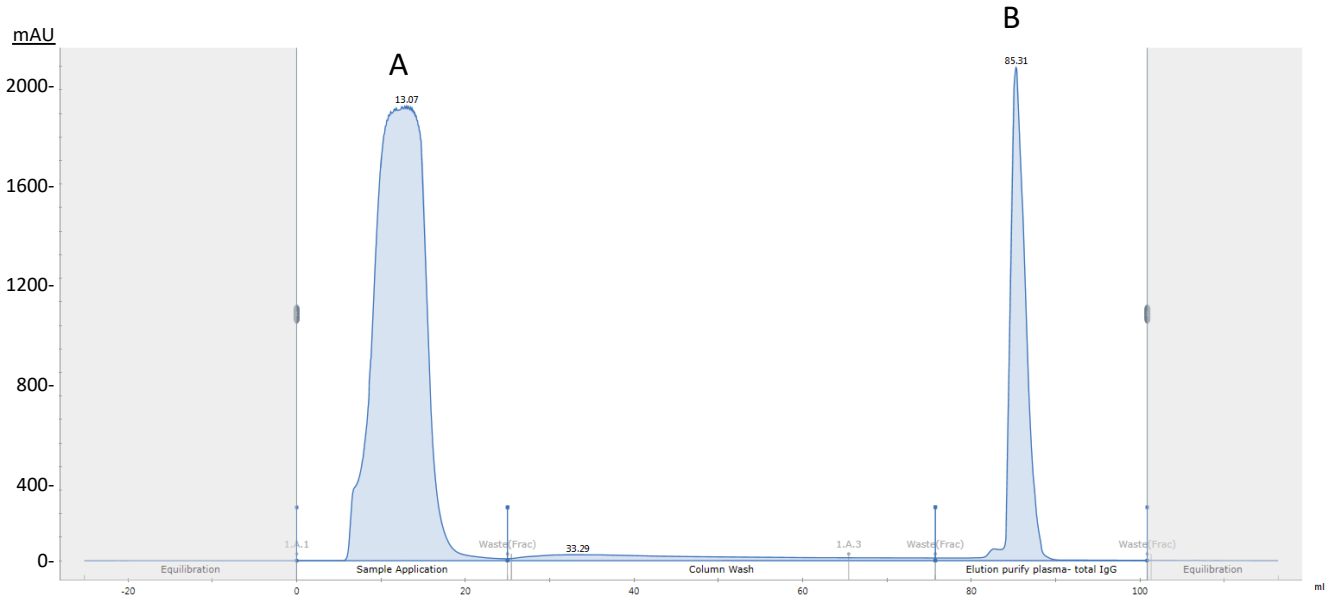

Figure 7. Purification of polyclonal IgG alpaca antibodies. Isolation from alpaca animal 1 day 0 using Fast Performance Liquid Chromatography (FPLC). Point A indicates unbound plasma protein discarded in the flow-through, and Point B is purified alpaca PcIgG.

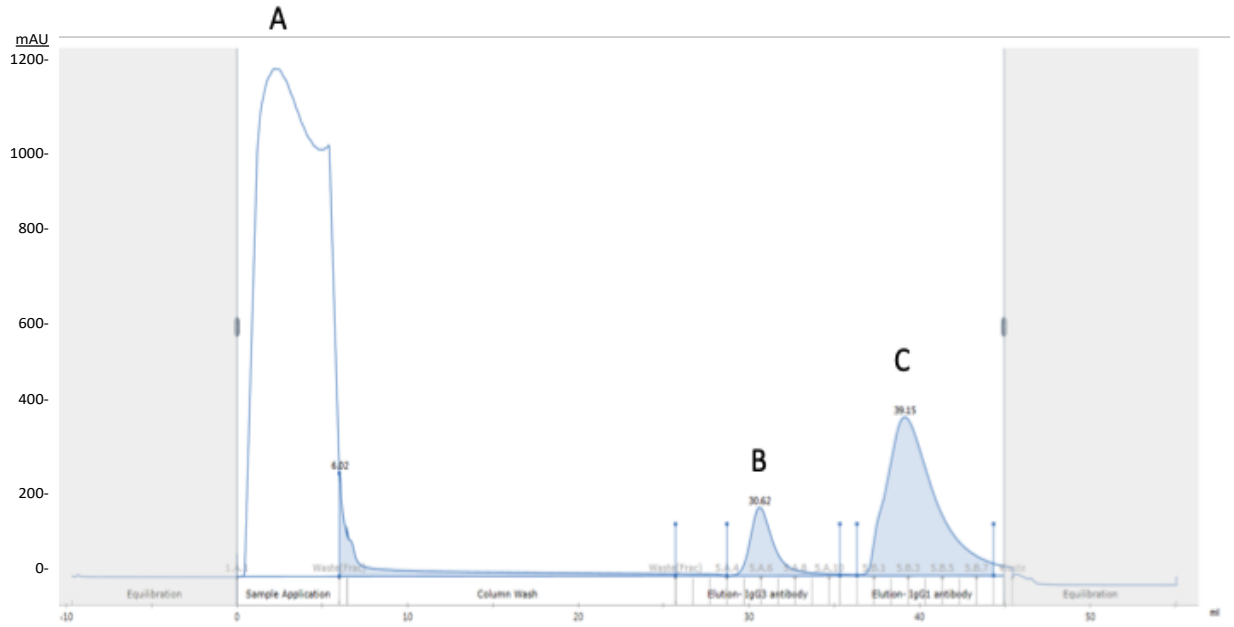

Figure 8. **Purification of alpaca IgG$_1$ and IgG$_3$.** Isolation of alpaca IgG$_1$ (point C) and IgG$_3$ (point B) antibodies from alpaca animal 1 day 0 plasma using Protein G column-based FPLC purification. Point A indicates unbound protein collected in flow-through.

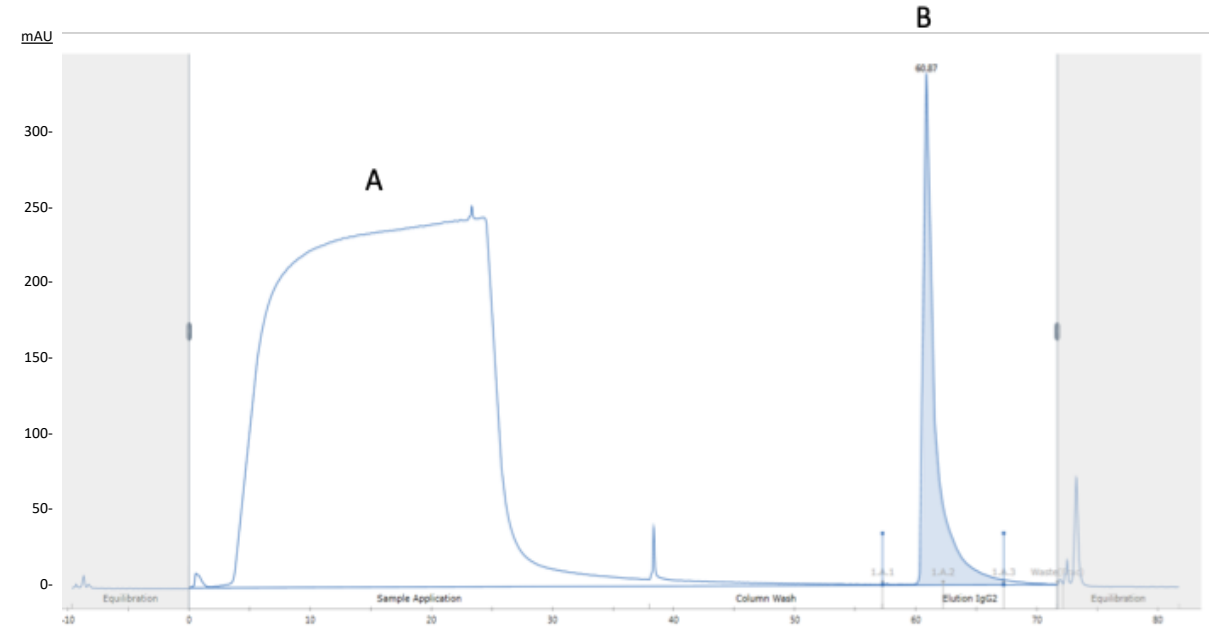

Figure 9. Purification of alpaca IgG$_2$. Isolation of alpaca IgG$_2$ (point B) antibodies from alpaca animal 1 day 0 plasma using Protein A column-based FPLC purification. Point A indicates unbound protein discarded in flow-through.

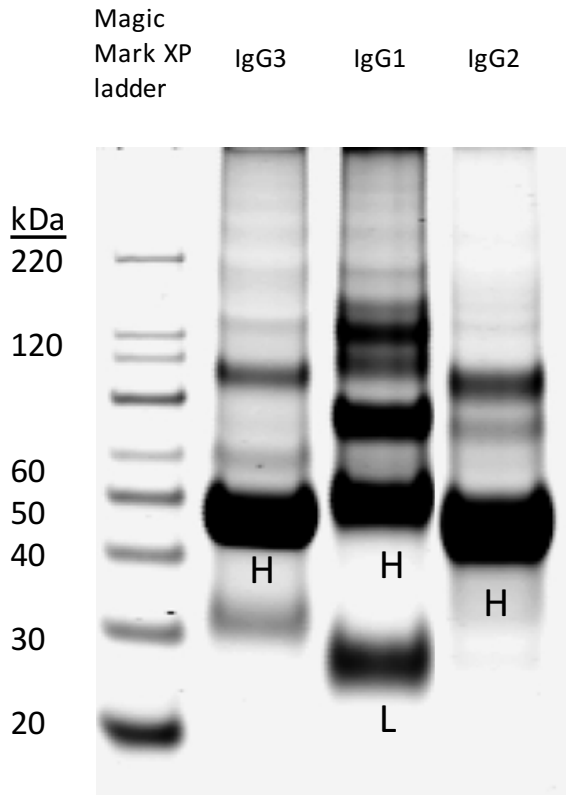

Figure 10. Analysis of purified alpaca IgG subtypes. Simplyblue Safe Stain protein gel of alpaca IgG subtypes isolated using FPLC.

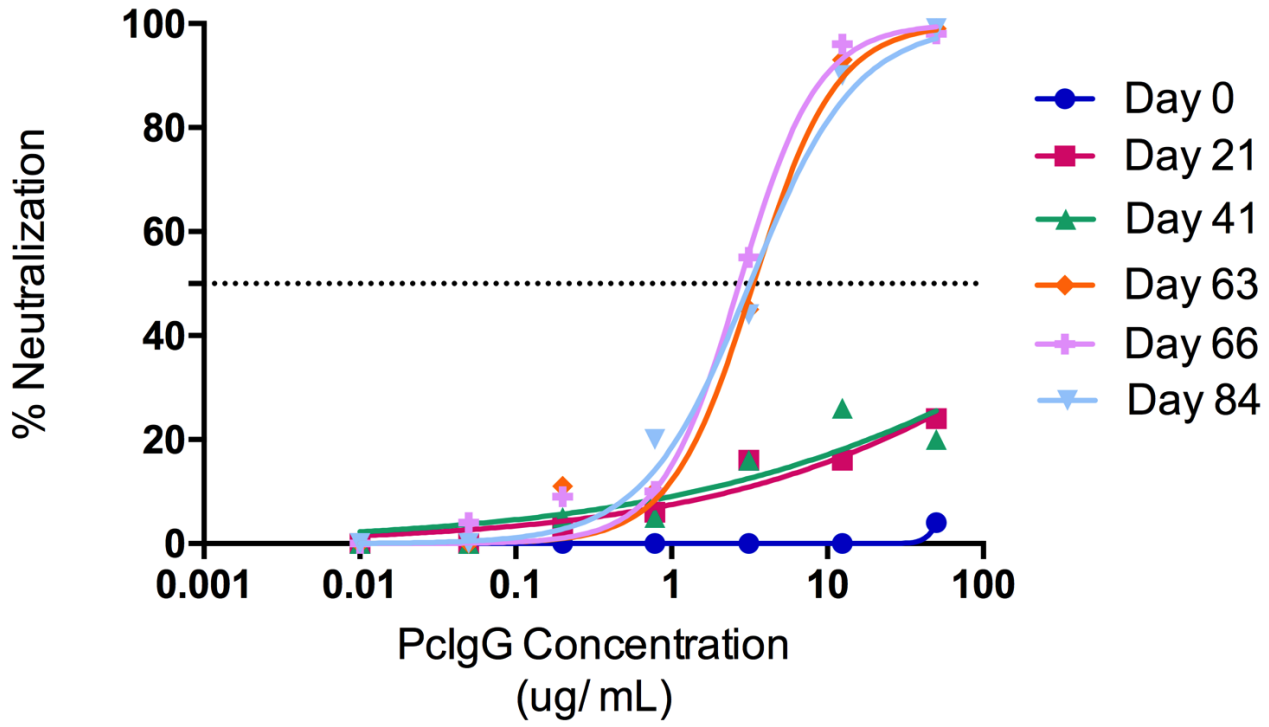

Figure 11. Purified PcIgG PRNT analysis from alpaca plasma. PcIgG neutralization analysis of alpaca plasma (animal 1) at blood collection time points. Vaccines were administered at days 0, 21, 41, and 63 after blood collections.

Table 2. Estimated EC_{50} values for purified PcIgG and IgG subtypes from alpaca animal 1 plasma collections.

Blood/ Plasma Collection Date	Antibody Subtype	EC_{50} Value (µg/ml)
Day 63	PcIgG	3.36
	IgG1	3.67
	IgG2	12.08
	IgG3	2.14
Day 66	PcIgG	2.73
	IgG1	4.78
	IgG2	38.54
	IgG3	0.83
Day 84	PcIgG	3.19
	IgG1	4.94
	IgG2	N/A
	IgG3	1.39

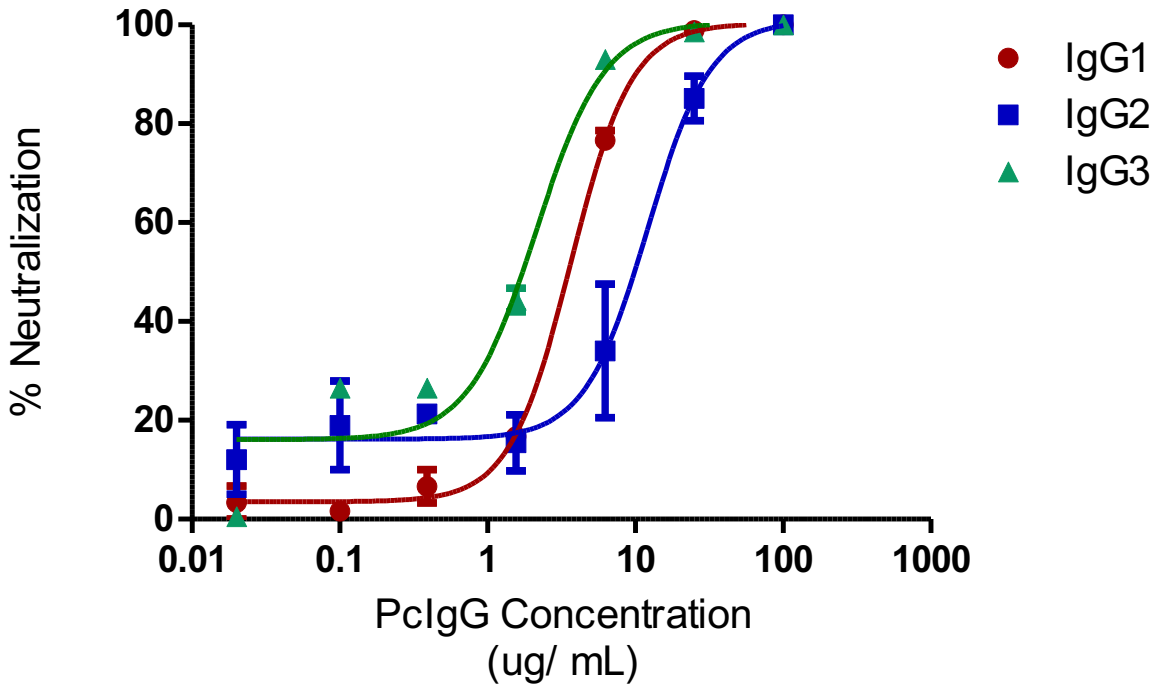

Figure 12. PRNT analysis of alpaca IgG subtypes (Day 63). Alpaca animal 1 day 63 purified IgG PRNT assay. Percent neutralization was determined by comparing sample wells to a VSV-ANDV control well and calculating the % reduction of plaques.

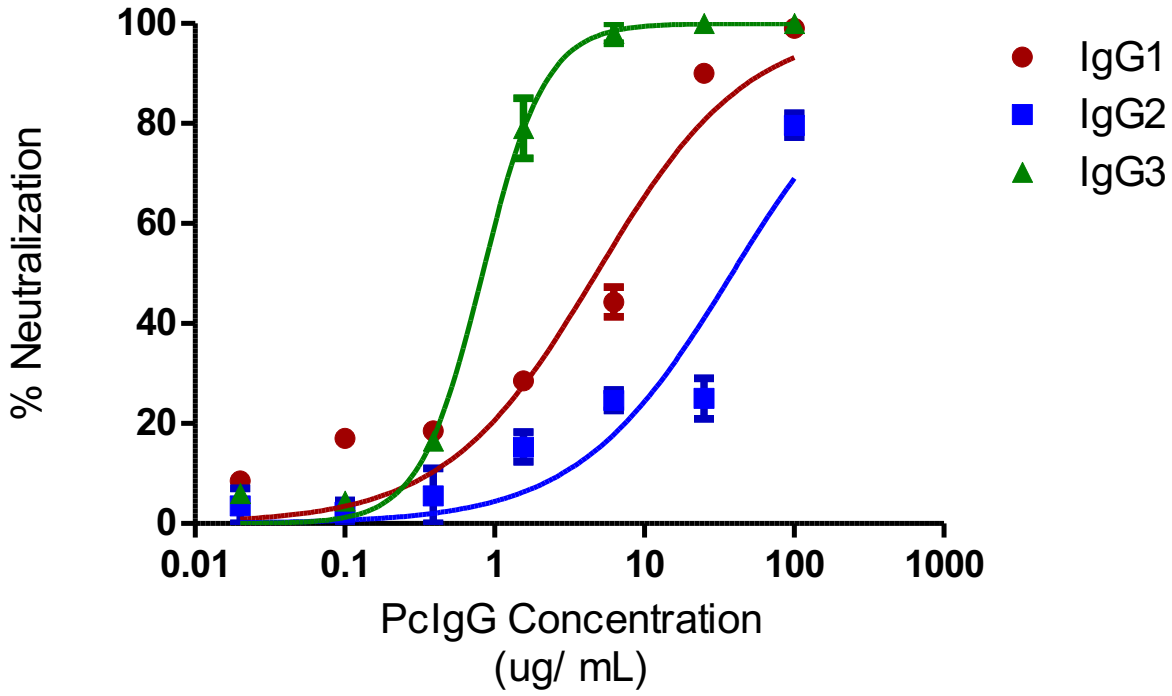

Figure 13. PRNT analysis of alpaca IgG subtypes (Day 66). Alpaca animal 1 day 66 purified IgG PRNT assay. Percent neutralization was determined by comparing sample wells to a VSV-ANDV control well and calculating the % reduction of plaques.

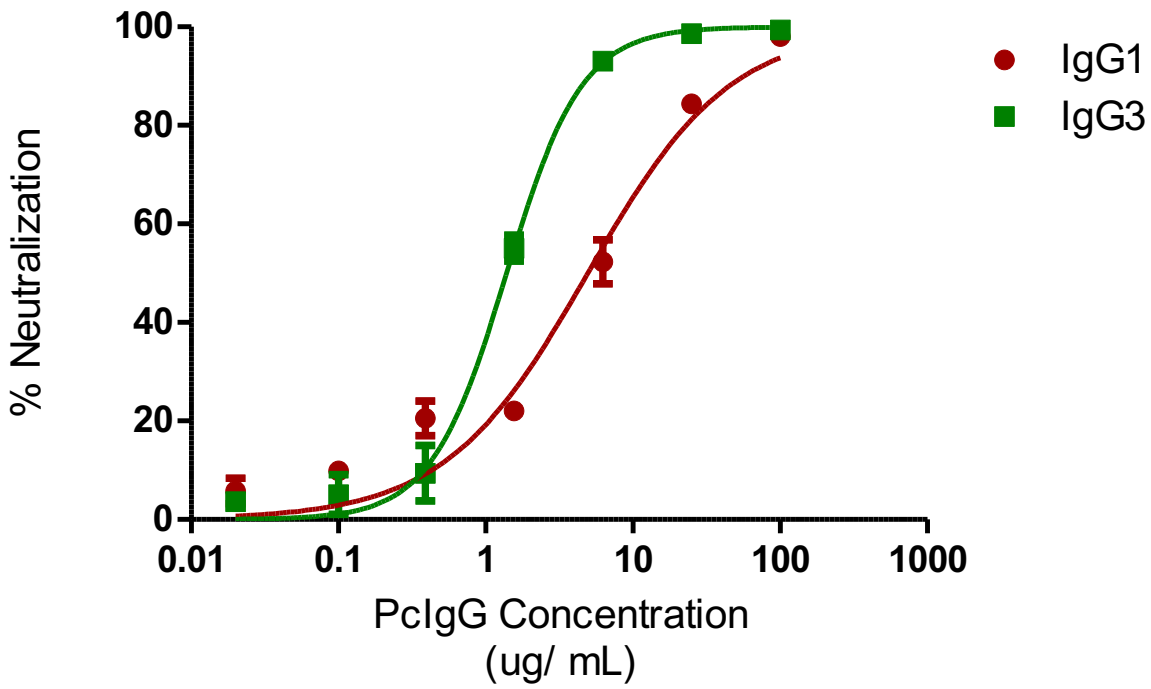

Figure 14. PRNT analysis of alpaca IgG subtypes (Day 84). Alpaca animal 1 day 84 purified IgG PRNT assay. Percent neutralization was determined by comparing sample wells to a VSV-ANDV control well and calculating the % reduction of plaques.

3.4 Bioavailability of polyclonal Alpaca IgG in hamsters

3.4.1 Rationale

Alpaca antibodies have been evaluated in multiple animal models, however they have not been examined in regards to the lethal Golden Syrian hamster model for ANDV [92,95,117]. Prior to determining the potential protective efficacy of alpaca antibodies against lethal ANDV infection, it is important to determine how long they remain within the blood stream of Golden Syrian hamsters. We propose to administer 100 mg/kg of purified PcIgG to each of 4 Syrian hamsters and collect blood at the following time points for analysis: 6, 24, 48, 72, 96, 120, 144, and 168 hours post treatment. The concentration of PcIgG at various time points will be extrapolated through comparison with known concentrations of PcIgG using a standard curve. Based on bioavailability studies in mice, we hypothesize that PcIgG will be detected within the blood of Golden Syrian hamsters 7 days (168 hours) after treatment administration [95].

3.4.2 Objective

Evaluate the bioavailability of purified alpaca PcIgG within the Golden Syrian hamster model. Serum levels of PcIgG will be assessed at various time points up to 7 days after a single administration of PcIgG.

3.4.3 Results

The objective for this experiment was to evaluate the length of time alpaca IgG antibodies remain in the blood stream within the Golden Syrian hamster model. As described in section 3.3.2, alpaca IgG antibodies were purified from alpaca plasma from animal 1 at the day 270 time point (section 2.2.8). Each hamster received 100 mg/kg of purified PcIgG

subcutaneously (section 2.2.9). The standard curve established using methods described in section 2.2.9.2 provided us with the means of determining the concentration of PcIgG within the hamster blood collections (Figure 15). Based on calculated concentration values of each collection using GraphPad Prism software, peak IgG detection in each hamster occurs at about 24 hours post-treatment ranging from 10 μg/ml to 18 μg/ml (Figure 16). After 24 hours the PcIgG concentration drops, and plateaus from 70 to 100 hours, then continues to decrease until 168 after PcIgG administration. At the final collection point of hour 168, ~40-60% of alpaca IgG was still present within the hamster bloodstream.

3.4.4 Summary

After 7 days, roughly ~40-60% of alpaca IgG is still detectable within the blood stream of Golden Syrian hamsters. The fairly long elimination time for alpaca PcIgG is ideal for a treatment, and its protective capabilities will be investigated in a future animal challenge experiment.

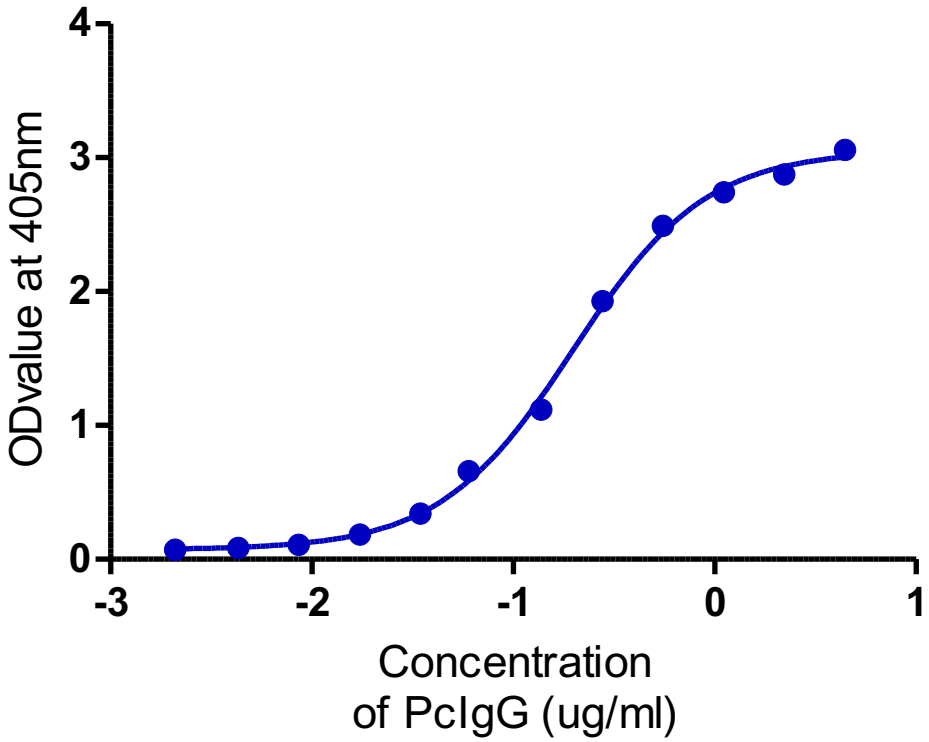

Figure 15. PcIgG standard curve. Standard curve of alpaca Polyclonal IgG antibodies from alpaca animal 1 at day 270 using ELISA. Standard curve values were graphed using GraphPad Prism software (X= log X non-linear curve).

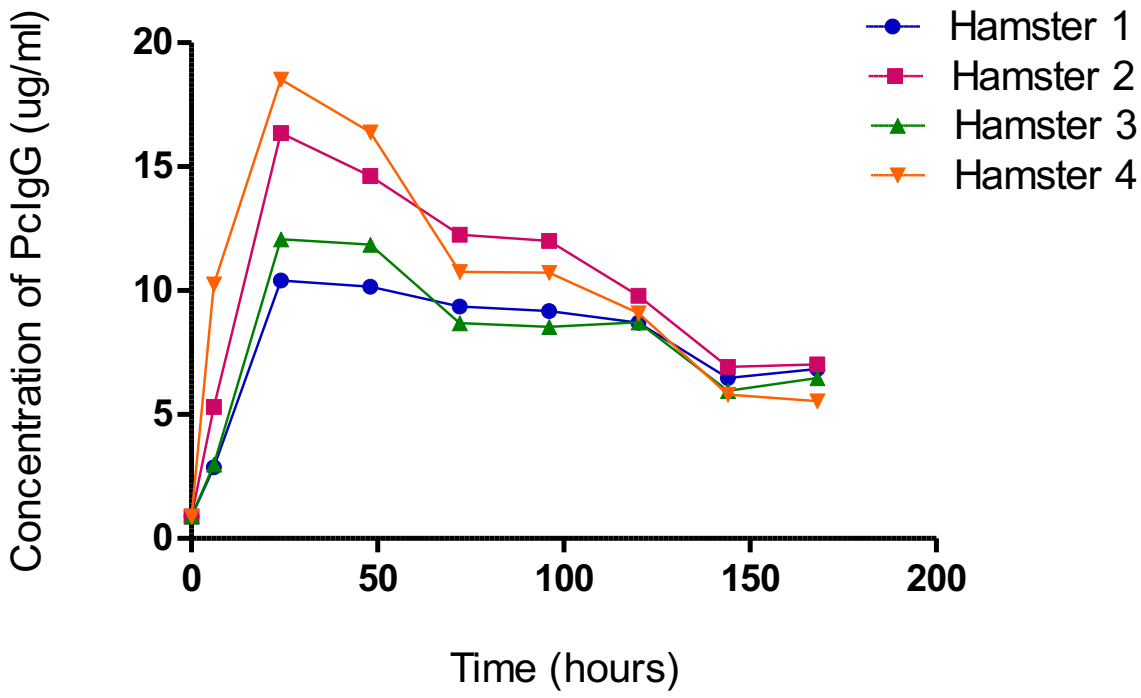

Figure 16. Bioavailability analysis of polyclonal alpaca IgG in the Syrian hamster model. Each animal received 100 mg/kg of purified PcIgG, with blood collections at the following time points: 6, 24, 48, 72, 96, 120, 144, and 168 hours post treatment. Polyclonal alpaca IgG concentrations were extrapolated by transforming OD values (obtained from ELISA) and comparing against interpolated X replicate values from the standard curve.

3.5 Therapeutic Evaluation of Alpaca PcIgG against Andes Virus Challenge

3.5.1 Rationale

Past animal protection studies involving ANDV have demonstrated success with using immune plasma as a source of treatment [72–75]. Neutralizing antibodies, targeting the surface glycoproteins G_n and G_c, are able to protect against lethal challenge within the Golden Syrian hamster model when administered early post infection [72–74]. Prior to conducting a protection study, we have established that using a DNA-based vaccine successfully results in the production of high-titre neutralizing antibodies within alpacas (Figure 6). Additionally, alpaca PcIgG antibodies are gradually eliminated from the bloodstream of the Golden Syrian hamster, with approximately 40-60% still present at 7 days post administration (Figure 16). Thus, we propose to examine the protective efficacy of ANDV-neutralizing PcIgG alpaca antibodies within the animal model as a possible treatment option. The treatment study will involve 3 groups of animals, each given their respective treatments at days +1 and +3 post challenge as stated in section 2.2.13. All animal manipulations will be conducted under ACC approved guidelines. The overall hypothesis for this study is that ANDV-neutralizing PcIgG alpaca antibodies will provide complete protection from lethal infection within the Golden Syrian hamster model.

3.5.2 Objective

Evaluate the protection of a neutralizing alpaca PcIgG antibody treatment against lethal ANDV challenge within the Golden Syrian hamster model. This will be conducted by a proof of concept animal study, where animals will be challenged with a lethal dose of ANDV and treated post-exposure with the purified alpaca PcIgG treatment.

3.5.3 Results

The objective of this experiment was to determine whether ANDV-neutralizing alpaca PcIgG antibodies would provide protection against lethal challenge within the Golden Syrian hamster model. As described in section 2.2.13, 27 animals were used and separated into three groups. Each animal received either neutralizing PcIgG treatment (from animal 1 day 270 collection), naïve antibody (non-neutralizing) treatment (day 0 collection), or PBS at days +1 and +3 post infection subcutaneously. Tissues collected from day 6 (section 2.2.14) were obtained and extracted RNA was evaluated using RT-qPCR. Results from the day 6 tissue collections show a significant difference regarding the viral load present between each group. Animals treated with neutralizing PcIgG have an average of 5 log genome copies/ml in the serum and lung, compared to the PBS and naïve-PcIgG treated groups which have approximately 8 log genome copies/ml (Figure 17). An even more remarkable difference is seen in the liver, heart, and kidney tissues, where the viral load in the neutralizing PcIgG treated animals is approximately 2 log genome copies/ml, and 6-8 log genome copies/ml in the PBS and naïve PcIgG treated groups. Looking at the level of survivors within each group (Figure 18), as expected all animals treated with PBS succumbed to disease by day 8. However, all animals treated with neutralizing alpaca PcIgG survived. Only 1 animal treated with naïve alpaca PcIgG survived the challenge, while the rest of the group succumbed to disease by day 8.

3.5.4 Summary

The results from the treatment study are significant, demonstrating that alpaca ANDV-neutralizing PcIgG antibodies provide complete protection from lethal challenge within the Golden Syrian hamster model, when administered at days 1 and 3 post-infection.

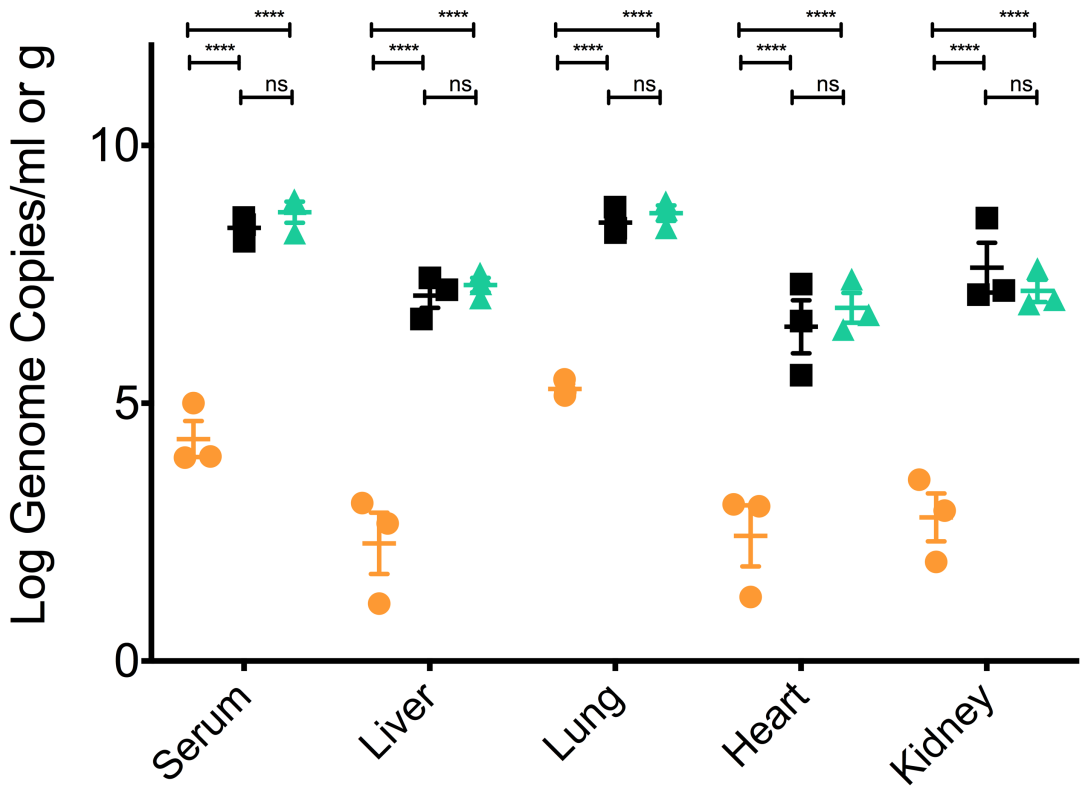

Figure 17. ANDV viral load detection within challenged Golden Syrian hamsters. Animals were treated with neutralizing alpaca PcIgG (orange), naïve alpaca PcIgG (green), or PBS (black). Results were graphed and compared using a Two-way Anova test, with multiple comparisons run using a Tukey's test. Bars with **** correspond to the sample groups being compared, and NS signifies not significant.

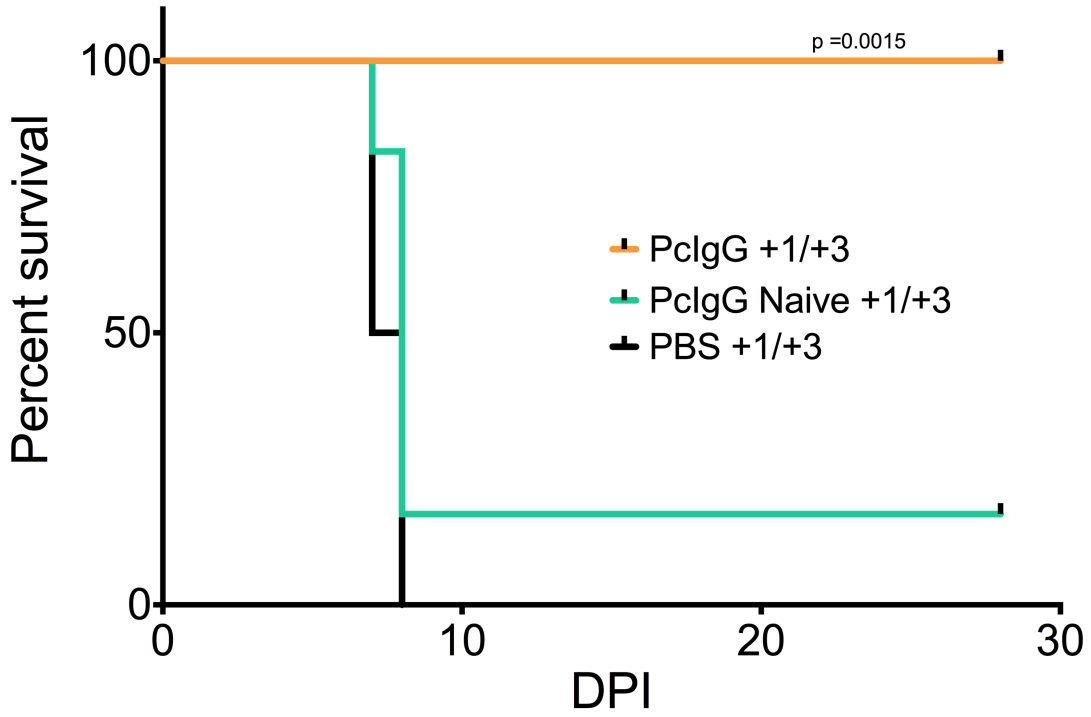

Figure 18. Survival curve of ANDV challenged Golden Syrian hamsters. Animals were treated with neutralizing alpaca PcIgG (orange), naïve alpaca PcIgG (green), or PBS (black). Survival analysis was conducted using a log rank Mantel-Cox test with a p value cut off of 0.05.

Chapter 4. Discussion

4.1 Alpaca Vaccine Preparation and Neutralizing Antibody Response

The primary objective of delivering an anti-viral vaccine is to induce the production of highly-specific neutralizing antibodies that will protect the individual if exposed to the pathogen. In regards to immunoglobulins, IgM is heavily involved in the innate system and is able to recognize viral markers [118,119]. The production of IgG, the immunoglobulin most effective for viral neutralization and responsible for long-lasting immunity, occurs later in the innate response with the maturation of naïve B cells [119]. B cells are incredibly important for the development of humoral immunity, as they produce highly-specific neutralizing antibodies that are able to efficiently bind foreign pathogens upon re-exposure [118]. Once a naïve B cell matures, these cells undergo clonal expansion and function as the immune system's long-lasting defense component, whereby during secondary exposure these cells produce abundant neutralizing IgG antibodies [118,119]. The pathway and responses mentioned above occur in the same way in response to vaccination, albeit the response is much more subdued.

As mentioned in the project rationale (section 1.9), the DNA vaccine encoding the ANDV glycoprotein precursor proteins was used to induce a humoral response within the alpacas, for the eventual production of highly-potent neutralizing anti-ANDV IgG antibodies. The vaccine was produced and prepared using The Qiagen Plasmid *Plus* Giga kits (Qiagen, Toronto, ON, Canada) (section 3.1.1), to yield enough vaccine for 3 alpacas during the vaccination schedule. To evaluate whether the DNA vaccine effectively expressed the ANDV glycoprotein sequence within the vaccine, each vaccine prep was evaluated initially

by transfecting 293T cells (section 3.1.2). The transfection reagent used in this experiment functioned to deliver the plasmid into the cells, where during cell division the plasmid would reach the nucleus, transcribe, and eventually become transiently expressed through the use of cell machinery. A positive pCAGGS-GFP control was also used and the transfection reaction was observed at 24, 48, and 72 hours to observe GFP expression. As seen in Figure 4, GFP expression was observed within the positive control at 24 hours, and steadily increased at the 48 hour and 72 hour time points. As the cells continued to divide, more and more copies of the plasmid were duplicated and therefore more expression is expected at later time points. At the 72 hour time point, cells transfected with the vaccine preps were lysed and the GPC protein was collected and visually examined through western blotting (section 3.1). Western blot was performed using ANDV specific primary antibodies. The glycoproteins are glycosylated, as mentioned by the name, with the Gn (GP1) having more glycosylation sites than the Gc (GP2) [120]. Glycosylation adds extra weight to the protein, interfering with its ability to migrate through the gel [121]. In addition, glycosylation interferes with the ability of SDS to work efficiently in denaturing the protein [121]. The vaccine preps, as mentioned in section 3.1, show ANDV glycoprotein expression in each transfection reaction with each vaccine prep (Figure 5). For the Gn (GP1) protein, two bands are seen corresponding to the glycosylated (71 kDa) and un-glycosylated form of the protein (~60 kDa). To confirm that ANDV-GPC was expressed within the DNA vaccine, we lysed transfected cells and collected the cell lysate mixture for western blot analysis (Methods 2.2.4). The faint glycosylated protein and the more pronounced un-glycosylated bands seen in Figure 5 for Gn (GP1) are likely attributed to the greater presence of un-glycosylated protein within the cell, as the glycoproteins are

transported to the Golgi and become glycosylated just prior to being transported to the cell membrane [37,38,43]. A faint band is seen for vaccine prep. 4 (Figure 5 A), which is possibly due to some of the sample spilling out of the well when it was loaded. For future measures a loading control with a known concentration, such as β-actin, such be loaded to ensure a consistent amount of protein is loaded in each well.

As mentioned in section 3.2, three alpacas were used in the vaccination study with the purpose of generating a high neutralizing antibody response. The vaccination study was designed so that each animal would receive 1 mg of the DNA vaccine administered with the Invivo-jet PEI adjuvant for aid in cellular delivery every 3 weeks. It is expected, as mentioned above, that the re-exposure to the GPC antigens from the vaccine would prompt the production of highly specific neutralizing IgG antibodies. Detection of neutralizing antibody levels through PRNT assays (section 3.2) reveal minimal or lack of neutralizing antibodies for the day 0 and day 21 collection points for all animals (Figure 6). This is expected as it takes time for a plasma cell population to develop, as B cells undergo maturation and the selected B cell population undergoes clonal expansion [118,119]. It isn't until prior to the third vaccine dose at day 41 that we see a detectable neutralizing antibody titre of roughly 1:40 to 1:80 with animal 1. At day 63, prior to the 4^{th} vaccine dose we see a jump in neutralizing antibody titre of roughly 1:1200 for animal 1, and roughly 1:80 for animal 3. At this stage, the plasma cell population has been developed and re-exposure to the viral GPC antigen from the vaccine will cause a quick and massive jump in neutralizing IgG antibody production. At the day 66 collection after 4 vaccine doses, the neutralizing antibody titre for animal 1 continues to jump to 1:2560, with animals 2 and 3

at roughly 1:40. For animal 2, the $PRNT_{80}$ titre dramatically jumps to 1:2560 at day 249 after receiving a boost.

This information proposes that the generation of a potent neutralizing antibody response takes time to develop and varies between animals. Having multiple vaccination points allows for multiple interactions to occur between antigen-presenting DC cells and B cells, which result in B cells processing the antigen and differentiating into antibody-producing plasma cells [122–124]. However, overtime only a small group of expanded B cells survive as long-term memory cells [122,123]. The additional vaccinations and boosts lead to the development of a quick and powerful humoral immune response, as seen with the high titres at days 66 and 84 with animal 1 (Figure 6A). The interesting finding within our experiment is the dramatic decrease in neutralization titres for animals 1 and 2 at day 270 (after receiving 2 boosts). Several possibilities can explain the fluctuation and eventual decrease in titres. First, the variation in response between all 3 animals during the vaccination course can be attributed to the animals being outbred. The strength in immune response will vary between each animal, explaining how animal 2 required a longer time to develop a similar neutralizing antibody response to animal 1. Second, a plateau phase was seen for animal 1 (at days 84, 249, and 270) and animal 2 (day 249 and 270). Immune responses typically plateau after several vaccinations, initially rising above the level of protection but then remaining near the protective threshold [122,123]. In addition, plateau phases have been seen for animal vaccination courses including alpacas where a maximum neutralization response was seen after several vaccinations [91,125]. For both animals 1 and 2, the neutralizing response plateaued at day 249 (after receiving a boost) and

dramatically dropped after the second boost as seen at day 270. One possible explanation for this drop in titre is that the majority of B-cells became unresponsive to the continuous stimulation. Limited information remains on this phenomenon, however a similar finding was seen linking boosts with hypo-responsiveness for meningococcus [123,126]. While immune responses do differ between viral antigens and bacterial polysaccharides, studies confirmed that B cells became hyporesponsive following a meningococcus vaccine boost in neonatal mice, leading to a lower neutralizing antibody response [123,126]. The exact mechanism of action is not yet defined, however these studies confirmed that the lack/ decrease in response is due to the eventual apoptosis of memory B-cells as a result of continuous stimulation [123,126]. In addition, the pool of memory cells was inhibited from being replenished as new B cells became unresponsive to the antigen presentation and failed to differentiate [123,126]. Whether or not a similar phenomenon occurred with regards to the alpaca vaccination is difficult to pinpoint, but a hyporesponsive behavior following a plateau phase certainly correlates to the findings in Figure 6.

As mentioned above, the lack of response with animal 3 can be attributed to the difference in immune response between the outbred animals. An attempt was made to induce a response by changing the boost administration from intradermal to intramuscular for days 228 and 249, however they proved to be unsuccessful. Purified proteins have been the common antigenic choice with regards to llama and alpaca vaccinations, therefore using DNA-vaccines may require additional boosts in order to see a high neutralizing response [95,97,111,127]. In addition, viruses tend to induce a stronger and quicker immune response than other vaccine forms [122,124,127]. For comparison, the study published by

Daley, L.P. *et al* used a formalin-inactivated virus as their vaccine source, and confirmed a high neutralizing response within each animal [91]. An additional reason for the variation in response is the adjuvant itself. For future work, several adjuvants should be investigated in order to determine the best candidate for alpaca vaccinations. Finally, investigating different vectors with different promoters could lead to optimization of protein expression. It would be helpful to compare immune responses in animals using different promoters, as successful *in vitro* protein expression does not guarantee the same result within the animal. One interesting approach to predicting the response of the animal to a vaccination would be to evaluate their response to past/previous vaccinations. A study published by Thompson, M.K. *et al* evaluated antibody responses using ELISA's in animals against commonly administered vaccines [127]. With their findings they were able to identify animals that produced a higher humoral antibody response, and are therefore predicted to respond more effectively to additional vaccinations [127]. This method could eliminate the cost, time, and resources used for future studies by selecting animals that are predicted to respond more favorably towards vaccinations.

4.2 Antibody Purification and PRNT Analysis

Aside from the slight difference in structure between the alpaca heavy-chain antibody subtypes, where IgG_1 possesses the conventional IgG structure and IgG_2 and IgG_3 are heavy-chain only, little is known about their difference in function. Isolation of each subtype is possible as each F_c domain interacts differently with protein A and protein G, isolated bacterial proteins that are used to coat liquid chromatography columns [90,103,116]. Alpaca IgG_1 (conventional) and IgG_3 (heavy-chain) bind both protein G and

protein A, while alpaca IgG_2 (heavy-chain) only binds to protein A [90,103,116]. The general principle behind PcIgG isolation is applying the prepared plasma to an equilibrated Protein A column, washing the column and removing any unbound protein (peak A of Figure 7), and collecting the PcIgG from the column by applying a low pH buffer (peak B of Figure 7). A similar principle is followed for obtaining each individual IgG subtype (section 2.8), however IgG_1 and IgG_3 is collected using Protein G columns while IgG_2 is obtained using Protein A columns (Figures 8 and 9). As seen from Figure 10, the purification method successfully obtained IgG_1 which has both a heavy and light chain. The subtypes IgG_2 and IgG_3 both have a heavy chain of approximately 42-45 kDa, as they lack a light chain (Figure 10). Additional bands are seen within each lane of the gel however, which indicates that additional steps could be taken to improve purity. For future purifications, buffer pH levels should be re-validated prior to the run to ensure that unspecific interactions are limited. In addition, a two-step purification method could be investigated to improve purity. However, the downside with additional steps is that a significant loss of sample may occur.

Past studies evaluating the production of neutralizing *Camelidae* heavy-chain IgG antibodies indicate that there are differences to the degree of neutralization and level of production [90,91]. When examining the protective antibody responses seen within alpacas when vaccinated against West Nile Virus (WNV), IgG_3 (heavy-chain) and IgG_1 (conventional) demonstrated similar neutralization levels using PRNT analysis [91]. In contrast, IgG_2 had the poorest neutralizing activity out of the three IgG subtypes, however enhanced neutralization activity was seen with the addition of complement proteins to the

assay [91]. It is unclear whether these results are virus-specific, so a similar analysis was conducted using the methods outlined in section 2.26-2.2.8. Evaluating purified PcIgG at different time points, we see that levels of neutralization increase after each vaccination (Figure 11). Additional information obtained from these experiments were the EC_{50} values, which relate to the amount of antibody required to see 50% of the maximum neutralization response. The EC_{50} value is applied to the strength of neutralization activity, where a lower value indicates that less antibody is required to see 50% neutralization. The determined EC_{50} values show a decrease in EC_{50} (from 3.36 ug/ml to 2.73 ug/ml) after animal 1 received the 4^{th} vaccination at day 63. After a 3 week period, the EC_{50} value increases from 2.73 ug/ml to 3.19 ug/ml at day 84. This information signifies that vaccinations successfully induce the production of neutralizing antibodies within the animal. To further evaluate the difference in subtype neutralization levels in regards to ANDV virus, PRNT analysis of purified IgG antibodies from day 63 (after 3 vaccinations) show that IgG_3 has the lowest EC_{50} value while IgG_2 has the highest and therefore lowest neutralization capacity (Figure 12 and Table 2). In addition, after the 4^{th} vaccination (day 66 collection) the EC_{50} value for IgG_3 decreased to 0.83 ug/ml while the IgG_2 value increased to 38.54 ug/ml (Figure 13 and Table 2). Again with the day 84 collection, IgG_3 continued to have a low EC_{50} value (Figure 14 and Table 2). Interestingly these results can be compared to what was examined with WNV, as IgG_3 remained the most potent neutralizing antibody, IgG_1 had potent neutralizing capabilities comparable to IgG_3, and IgG_2 proved to have the worst neutralizing capabilities [91].

4.3 Bioavailability of PcIgG Alpaca Antibodies

The use of *Camelidae* IgG antibodies as therapeutics is a fairly new development, and there is limited information regarding their bioavailability in animal models. Humanized heavy-chain alpaca IgG antibodies have a half-life of approximately 5 days within mice, however their bioavailability within the Golden Syrian hamster model is unknown [95]. With the experiment outlined in section 2.2.11, hamsters received 100 mg/kg of purified PcIgG alpaca antibodies and blood was collected every 24 hours for 7 days. Detection of alpaca IgG antibodies through ELISA's reveal that peak detection of antibodies occurs at roughly 24 hours post injection, and steadily decreased over the next 7 days (Figure 16). Interestingly, approximately 50% of antibodies remain in the bloodstream within Golden Syrian hamsters at day 7 (Figure 16). Bioavailability is an important factor when evaluating possible treatment candidates, as a short time would require continuous treatment administration. In regards to ANDV, potentially exposed patients are typically seen by a healthcare professional during onset of symptoms and during the cardiopulmonary phase. Having a treatment with a long bioavailability would be critical for ANDV, as it could be administered during the onset of symptoms and still remain within the body over the next week when the cardiopulmonary phase is expected to begin. For future purposes, the collection points should be extended for a further 2 weeks to determine the exact time that PcIgG is cleared from the Golden Syrian hamster. Additional time points would additionally allow us to determine the exact half-life of alpaca PcIgG antibodies within the ANDV hamster model.

4.4 Protective efficacy of PcIgG Alpaca Antibodies

As past studies have successfully demonstrated that neutralizing antibodies can be used to treat ANDV infections within Golden Syrian hamsters, our objective was to evaluate whether neutralizing alpaca PcIgG antibodies could produce the same result [66,73,74]. The hamster model typically succumbs to ANDV lethal infection at days 8-9, and past antibody treatments administered before days 5-6 have been successful at preventing disease [73–75,128]. Data from the bioavailability experiment (section 3.4) reveal that alpaca PcIgG antibodies are still significantly present within hamsters 1 week after administration (Figure 16). To determine the protective efficacy of alpaca PcIgG antibodies against lethal ANDV infection, alpaca serum from animal 1 at day 270 was purified, along with pre-bleed (day 0), using FPLC (section 2.2.8). Three groups of 9 hamsters were used in the study: one receiving naïve PcIgG, one receiving neutralizing PcIgG, and one receiving PBS. Each animal received 100 mg/kg of respective treatment at days +1 and +3 post challenge, as specified in section 2.2.13. The overall results show that each animal within the PBS group succumbed to disease, as expected, at days 7 and 8 (Figure 18). The hamsters treated with naïve PcIgG antibody died at days 7 and 8, with only one survivor within the group (Figure 18). It is not uncommon to have one or two animal survivors within the naïve antibody control group, as is seen with past studies [72,73]. One possible explanation for this is that receiving any form of antibody, neutralizing or not, causes the immune system to become heightened and therefore more aware of an infection. The most significant data is from the neutralizing PcIgG treated group, where all animals survived the challenge (Figure 18). RT-PCR analysis of tissues harvested from animals euthanized at day 6 post challenge reveal a difference in viral RNA levels between groups (Figure 17).

Neutralizing PcIgG antibodies significantly reduce viral load within hamster tissues. The PBS and naïve PcIgG treated groups show similar viral RNA levels, with approximately 8 log genome copies/ml in the serum and lung and 6-7 log genome copies/ml in the heart (Figure 17). This is in contrast to the neutralizing PcIgG treated group where viral RNA levels are much lower, with 5 log genome copies/ml in the serum and lung and approximately 2 log genome copies/ml in the heart and liver. These findings are comparable to what has been seen in previous studies, where the passive transfer of immune sera or administration of neutralizing antibodies protected hamsters from lethal ANDV infection [69,72–75,128]. Again this experiment focused on treating infected animals early in the disease course, therefore it would be interesting to see whether delaying the treatment course by several days would produce the same survival rate. One interesting point to consider for future experiments would be to collect serum from animals every day or every other day, as to determine the difference in viral RNA levels between groups throughout the experiment.

4.5 Contributions to the Field of Hantavirus and Antibody Therapy

A major issue in regards to the field of Hantaviruses is the lack of approved and effective treatments. A vaccination strategy for ANDV is not particularly feasible as the number of cases remains low in respect to current circulating global viruses. However, the high mortality rate combined with the person-to-person transmission and quick progression of HPS stresses the need for novel treatments [56,129,130]. The success of passive transfer studies indicates the vast potential of using neutralizing antibodies as a successful and potent treatment [67,72,74,128]. One problem however remains the narrow treatment

window, where treatment administered to infected hamsters past days 5/6 does not result in survival [67,72,74,128]. The focus of this thesis is to investigate the potential of using ANDV-neutralizing alpaca antibodies as a potential treatment for ANDV. From the experimental results, numerous findings can be applied to the field of Hantavirus. First and foremost, results from the protection study (Figures 17 and 18) indicate that indeed PcIgG alpaca antibodies provide complete protection from disease in the Golden Syrian hamster model when administered early post challenge. In addition, alpaca PcIgG significantly reduce viral load in tissues when compared to naïve treated or mock-treated animals (Figure 17). This is the first incidence where alpaca antibodies have been investigated as treatment sources for Hantaviruses.

Second, results from the IgG subtype PRNT analysis reveal that the most potent neutralizing activity comes from the heavy-chain IgG_3 (Table 2). This not only re-emphasizes the immense binding potential of alpaca heavy-chain antibodies, but provides a direction for future ANDV protection studies. Third, results gathered from the vaccination time course (Figure 6) provide additional information for animal vaccinations in general. The exact balance between the number of boosts and when to boost is important information as the objective is to induce a high titre neutralizing antibody response within the animal. What was seen after successive boosts is a plateau phase, where the neutralizing titre was at its highest point (day 249 of Figure 6). Afterwards, a decrease in neutralizing titre was observed suggesting a hypo-responsiveness of B cells towards the vaccine. Both a plateau phase and a hyporesponsive reaction has been noted in several vaccination studies, although the exact mechanisms of this remain debated [91,123,126,127]. Fourth,

the bioavailability study described in section 2.2.11 is the first conducted using alpaca antibodies for Golden Syrian hamsters. This information is applicable not only to the field of Hantavirus treatments and therapeutics, but adds additional information regarding the activity and absorption of *Camelidae* antibodies.

4.6 Major Findings, Concluding Remarks, and Future Directions

The central hypothesis, section 1.9, for this project is that DNA vaccination of alpacas against the ANDV glycoprotein will result in an immune response leading to the production of neutralizing IgG antibodies. Additionally, purified alpaca IgG antibody from vaccinated animals will provide protection against lethal ANDV challenge within the Golden Syrian hamster model. The findings from the experiments outlined in this study answer the objectives outlined in section 1.9:

1) Expression of ANDV-GPC within the pCAGGS-ANDV-GPC vaccine was successfully established through transfection and western blot analysis.
2) The DNA vaccine successfully induced neutralizing antibody production within alpaca's 1 and 2. PRNT analysis of alpaca plasma revealed that animal 1 responded to the first 4 vaccinations, whereas significant neutralizing antibody levels weren't observed in animal 2 until days 249 and 270. Animal 3 failed to respond to the vaccination schedule, even with the change in administration from intradermal to intramuscular.
3) PRNT analysis of animal 1 PcIgG reveals that alpaca PcIgG can successfully neutralize VSV-ANDV-GPC. In addition, analysis of days 63, 66, and 84

antibodies reveal that IgG_3 has the most potent neutralizing ability, whereas IgG_2 had the worst neutralizing activity of the alpaca subtypes.

4) The bioavailability study of alpaca PcIgG antibodies within the Golden Syrian hamster model reveal that peak alpaca PcIgG antibody concentration within blood is detected 24 hours post injection. In addition, approximately 50% of initial alpaca PcIgG is still detected within the hamster blood stream.
5) The proof of concept hamster protection study show that neutralizing PcIgG antibodies protect against lethal ANDV infection when administered at days +1 and +3 post infection. In addition, RT-PCR analysis reveal that neutralizing PcIgG antibodies significantly reduce viral load within tissues.

The major findings in the project reveal that alpaca IgG antibodies show great potential as a possible ANDV treatment. These results provide a base for the future directions of this project. Future work could examine multiple avenues. First, repeating the bioavailability study and increasing the collections, as well as increasing the length of the experiment, would allow for the determination of the half-life of alpaca PcIgG antibodies. Following this experiment, half-life determination of alpaca IgG_3 within the Golden Syrian hamster would be particularly interesting as IgG_3 possessed the strongest neutralization activity as concluded from the PRNT analysis. By determining the half-life, the optimal dosage of alpaca antibody could be calculated. The information gathered from the protection study described in section 2.2.13 above provides a baseline for future animal work. Additional protection studies, involving extending the therapeutic window or administering a single treatment dose, would provide more information regarding the ability for alpaca IgG

antibodies to inhibit ANDV disease. These protection studies could compare the protective efficacy of each individual subtype (IgG_1, IgG_2, IgG_3), versus PcIgG. The eventual path of this project would be to develop a highly-potent neutralizing V_{HH} nanobody, that could be delivered directly into the lungs using a nebulizer. The small size of the V_{HH} is an advantage when it comes to therapeutics, and currently a nebulized RSV nanobody treatment is in clinical trials for its potential as a safe and effective treatment [92,93,131–133]. The concept of delivering treatment directly into the lungs is particularly attractive for ANDV as the lungs and heart remain the primary target organs for the virus. Using the PBMC collected from animal 1 at day 66, the extracted RNA would be used to create a library of nanobody clones. Screening this library through phage display or Virus Neutralization Assay adapted methods would yield a list of candidates for ANDV treatment. The advantage of this *in vitro* method is that nanobodies can be produced in a variety of expression systems, such as bacteria and yeast, with minimal cost [92,93,131–133]. Using these potential treatment candidates, bioavailability experiments and protection studies would be conducted to determine their overall ability to inhibit disease. It would be particularly interesting to evaluate the level of protection by comparing subcutaneously delivered nanobodies versus nebulized nanobodies. Further manipulations may be required in order to optimize the treatment, such as comparing a monovalent, divalent, and trivalent nanobody treatment [92,93,131–133].

The results evaluated in this thesis contribute greatly to the field of Hantaviruses. With the limited number of treatments available for HPS, there is a growing need for the development of novel and effective therapeutics. The successful results obtained from our

protection study, as well as the additional neutralization and bioavailability information, provide a baseline and a positive outlook for future developments of an alpaca antibody ANDV treatment.

Chapter 5. Appendixes

APPENDIX A: Commercial Reagents:

Vaccine preparation

-Qiagen Plasmid *Plus* Giga Kit (Qiagen, Toronto, ON, Canada)

-Invivo-Jet PEI Transfection Reagent (VWR, Mississauga, ON, Canada)

ANDV GPC expression reagents and equipment

-X-tremeGENE™ HP DNA Transfection Reagent (Sigma- Aldrich, Oakville, ON, Canada)

-HyClone™ Dulbecco's Modified Eagles Medium (Fisher Scientific, Ottawa, ON, Canada)

-HyClone™ Penicillin Streptomycin (100X) Solution (Fisher Scientific, Ottawa, ON, Canada)

-HyClone™ Fetal Bovine Serum (Fisher Scientific, Ottawa, ON, Canada)

-Gibco™ Opti-MEM™ Reduced Serum Medium (Fisher Scientific, Ottawa, ON, Canada)

-EVOS M5000 Imaging System (Fisher Scientific, Ottawa, ON, Canada)

ANDV GPC Western Blot reagents and equipment

-QIAshredder homogenizers (Qiagen, Toronto, ON, Canada)

-Bolt™ (4X) LDS Sample Buffer (Fisher Scientific, Ottawa, ON, Canada)

-Ambion™ Nuclease-Free Water (Fisher Scientific, Ottawa, ON, Canada)

-Bolt™ 4-12% Bis-Tris Plus Gels (Fisher Scientific, Ottawa, ON, Canada)

-NuPAGE™ MES SDS Running Buffer (20X) (Fisher Scientific, Ottawa, ON, Canada)

-MagicMark™ XP Western Protein Standard (Fisher Scientific, Ottawa, ON, Canada)

-Invitrogen Mini Gel Tank (Fisher Scientific, Ottawa, ON, Canada)

-iBlot®2 Dry Blotting System (Fisher Scientific, Ottawa, ON, Canada)

-iBlot®2 NC Mini Stacks (Fisher Scientific, Ottawa, ON, Canada)

-Mouse Monoclonal Anti-Glycoprotein C of Andes Virus IgG fraction (AMSBIO LLC, Cambridge, MA, USA)

-Mouse Monoclonal Anti-Glycoprotein N of Andes Virus IgG fraction (AMSBIO LLC, Cambridge, MA, USA)

-IRDye 800CW Goat anti-Mouse IgM (0.5mg) (Cedarlane, Burlington, ON, Canada)

-Tween™ 20 (Fisher Scientific, Ottawa, ON, Canada)

-Odyssey® Blocking Buffer (PBS) (LI-COR Inc., Lincoln, NE, USA)

-Li-Cor® Odyssey Imaging System (LI-COR Inc., Lincoln, NE, USA)

-Nanodrop™ One Microvolume UV-Vis Spectrophotometer (Fisher Scientific, Ottawa, ON, Canada).

FPLC Antibody Purification Reagents and Equipment

-HiTrap Protein A HP columns (1ml and 5ml) (GE Healthcare, Mississauga, ON, Canada)

-HiTrap Protein G HP columns (1ml and 5ml) (GE Healthcare, Mississauga, ON, Canada)

-AKTA Pure Protein Purification System (GE Healthcare, Mississauga, ON, Canada)

-Gibco™ Phosphate Buffered Saline pH 7.2 (1X) (Fisher Scientific, Ottawa, ON, Canada)

-Pierce™ Protein Concentrator PES 10K MWCO (2-6 ml, 5-20ml) (Fisher Scientific, Ottawa, ON, Canada)

Alpaca IgG Protein Gel Reagents

-MagicMark™ XP Western Protein Standard (Fisher Scientific, Ottawa, ON, Canada)

-Bolt™ (4X) LDS Sample Buffer (Fisher Scientific, Ottawa, ON, Canada)

-Ambion™ Nuclease-Free Water (Fisher Scientific, Ottawa, ON, Canada)

-Bolt™ 4-12% Bis-Tris Plus Gels (Fisher Scientific, Ottawa, ON, Canada)

-NuPAGE™ MES SDS Running Buffer (20X) (Fisher Scientific, Ottawa, ON, Canada)

-Invitrogen Mini Gel Tank (Fisher Scientific, Ottawa, ON, Canada)

-SimplyBlue™ SafeStain (Fisher Scientific, Ottawa, ON, Canada)

Animal Cell Culture Reagents

-HyClone™ Dulbecco's Modified Eagles Medium (Fisher Scientific, Ottawa, ON, Canada)

-HyClone™ Penicillin Streptomycin (100X) Solution (Fisher Scientific, Ottawa, ON, Canada)

-HyClone™ Fetal Bovine Serum (Fisher Scientific, Ottawa, ON, Canada)

Plaque Reduction Neutralization Test (PRNT) Reagents

-HyClone™ Dulbecco's Modified Eagles Medium (Fisher Scientific, Ottawa, ON, Canada)

-HyClone™ Penicillin Streptomycin (100X) Solution (Fisher Scientific, Ottawa, ON, Canada)

-HyClone™ Fetal Bovine Serum (Fisher Scientific, Ottawa, ON, Canada)

-UltraPure™ L.M.P. Agarose (Low Melting Point) (Fisher Scientific, Ottawa, ON, Canada)

-Crystal Violet Biological Stain (Sigma- Aldrich, Oakville, ON, Canada)

Reverse Transcriptase PCR Reagents and Equipment

-RLT lysis buffer (Qiagen, Hilden, Germany)

-RNeasy mini kit (Qiagen, Hilden, Germany)

-Viral RNA mini kit (Qiagen, Hilden, Germany)

-Quantstudio3 Real Time PCR System (Fisher Scientific, Ottawa, ON, Canada)

ELISA Reagents and Equipment

-Corning Costar Assay Plate, 96 well Flat Bottom (Corning, USA)

-Difco™ Skim Milk Powder (VWR, Mississauga, ON, Canada)

-Goat anti-llama IgG (H+L) Secondary Antibody HRP-conjugated A16060 (Fisher Scientific, Ottawa, ON, Canada)

-Tween™ 20 (Fisher Scientific, Ottawa, ON, Canada)

-ABTS Peroxidase Substrate A and B solution (VWR, Mississauga, ON, Canada)

-Synergy HTX Multi-Mode Reader (Biotek, VT, USA)

APPENDIX B: Laboratory-made Reagents:

General Laboratory Buffers

All materials were purchased from Sigma-Aldrich (Oakville, ON, Canada) or Fisher Scientific (Ottawa, ON, Canada) unless otherwise stated.

-Phosphate Buffered Saline, pH 7.4

-8g of NaCl

-0.2g of KCl

-1.44g of Na_2HPO_4

-0.24g of KH_2PO_4

-Adjust the pH to 7.4 with HCl, autoclave

-Protein Denaturing Buffer

-50mM HEPES 8.8

-100mM DTT

-Fill to 4mL with 4% SDS

-Western Blot Running Buffer

-50mL NuPAGE™ MES SDS Running Buffer (20X)

-Fill to 1L with RO water

-Western Blot Wash Buffer

-1L of laboratory prepared PBS pH 7.4

-1mL of Tween 20

-Western Blot Blocking Reagent

-20mL of Odyssey® Blocking Buffer (PBS) (LI-COR Inc., Lincoln, NE, USA)

-20mL of laboratory prepared PBS pH 7.4

-Western Blot Antibody Diluent

-20mL of Odyssey® Blocking Buffer (PBS) (LI-COR Inc., Lincoln, NE, USA)

-20mL of laboratory prepared PBS pH 7.4

-0.2% Tween 20

-Alpaca IgG_3 Elution Buffer

-0.15M NaCl

-0.58% Acetic Acid

-Fill to 1L with ddH_20

-Adjust pH to 3.5, filter sterilize with 0.22µM filter

-Alpaca Polyclonal IgG/ IgG1 Elution Buffer

-0.1M glycine-HCl

-Fill to 1L with ddH_2O

-Adjust pH to 2.7, filter sterilize with 0.22µM filter

-Alpaca IgG_2 Elution Buffer

-0.15M NaCl

-0.58% Acetic-acid

-Fill to 1L with ddH_2O

-Adjust pH to 3.5, filter sterilize with 0.22µM filter

-HiTrap Protein A and G Column Binding Buffer

-20mM Sodium Phosphate

-Fill to 1L with ddH_2O

-Adjust pH to 7.0, filter sterilize with 0.22µM filter

-Antibody Stabilizing Buffer

-1M Tris-HCl

-Fill to 1L with ddH_2O

-Adjust pH to 9.0, filter sterilize with 0.22µM filter

-20% NaCl SafeBlue Stabilizing Buffer

-20g NaCL

-Fill to 1L with ddH_2O

-Autoclave

-2% LMP Agarose

-10g of UltraPure™ L.M.P. Agarose

-Fill to 500mL with RO water

-Autoclave, aliquot 20mL into 50mL Falcon tubes

-Crystal Violet Stock Solution

-2% Crystal Violet (w/v)

-100mL EtOH (100%)

-50mL 37% Formaldehyde Solution

-Fill to 1L with RO water

-Crystal Violet Working Solution

-100mL Crystal Violet Stock solution

-100mL 37% Formaldehyde

-Fill to 1L with RO water

<u>Bacterial Cell Culture</u>

-LB Miller + 100 μg/mL Ampicillin broth

-10grams Bacto-tryptone

-5grams Bacto-yeast extract

-10grams NaCl

-Fill to 1L with ddH_20, autoclave

-Add 0.1grams of Ampicillin

-LB Miller + 100 µg/mL Ampicillin agar plates

-Add 20grams of agar to the above recipe

-Fill to 1L with ddH_20

-Autoclave and let cool down to ~60^0C.

-Add 0.1grams of ampicillin

-Pour into sterile petri plates

Animal Cell Culture

-Supplemented DMEM medium

-500mL HyClone™ Dulbecco's Modified Eagles Medium (Fisher Scientific, Ottawa, ON, Canada)

-50mL of HyClone™ Fetal Bovine Serum (Fisher Scientific, Ottawa, ON, Canada), heat inactivated.

-5mL of HyClone™ Penicillin Streptomycin (100X) Solution (Fisher Scientific, Ottawa, ON, Canada)

Chapter 6. References

1. Lee HW, Vaheri A, Schmaljohn CS. Discovery of hantaviruses and of the Hantavirus genus: Personal and historical perspectives of the Presidents of the International Society of Hantaviruses. *Virus Res.* 187, 2–5 (2014).
2. Clement J, Maes P, Van Ranst M. Hemorrhagic Fever with Renal Syndrome in the New, and Hantavirus Pulmonary Syndrome in the old world: Paradi(se)gm lost or regained? *Virus Res.* 187, 55–58 (2014).
3. Clement J, Maes P, Van Ranst M. Hantaviruses in the Old and New World. Perspect. Med. Virol.16, 161–177 (2006).
4. Schmaljohn C, Hjelle B. Hantaviruses: A Global Disease Problem. *Emerg. Infect. Dis.* (1997).
5. Clement J. Hantavirus. In: *Emergency Management of Infectious Diseases*, Cambridge University Press, 469–474 (2003).
6. Jonsson CB, Figueiredo LTM, Vapalahti O. A global perspective on hantavirus ecology, epidemiology, and disease. Clin. Microbiol. Rev.23(2), 412–441 (2010).
7. Souza WM, Bello G, Amarilla AA, Alfonso HL, Aquino VH, Figueiredo LTM. Phylogeography and evolutionary history of rodent-borne hantaviruses. *Infect. Genet. Evol.* [Internet]. 21, 198–204 (2014). Available from: http://dx.doi.org/10.1016/j.meegid.2013.11.015.
8. Zhang YZ, Holmes EC. What is the time-scale of hantavirus evolution? *Infect. Genet. Evol.* [Internet]. 25, 144–145 (2014). Available from: http://dx.doi.org/10.1016/j.meegid.2014.04.017.
9. Avšič Županc T, Korva M. Hantavirus Infections. In: *Emerging Infectious*

Diseases: Clinical Case Studies, Elsevier Inc., 25–36 (2014).

10. Peters, MD CJ, Simpson, MD, PhD, MPH GL, Levy, MD, PhD H. SPECTRUM OF HANTAVIRUS INFECTION: Hemorrhagic Fever with Renal Syndrome and Hantavirus Pulmonary Syndrome. *Annu. Rev. Med.* 50(1), 531–545 (2002).
11. Kim YK, Lee SC, Kim C, Heo ST, Choi C, Kim JM. Clinical and laboratory predictors of oliguric renal failure in haemorrhagic fever with renal syndrome caused by Hantaan virus. *J. Infect.* 54(4), 381–386 (2007).
12. Pensiero MN, Sharefkin JB, Dieffenbach CW, Hay J. Hantaan virus infection of human endothelial cells. *J. Virol.* 66(10), 5929–5936 (1992).
13. Clement J, Leduc JW, McElhinney LM, Reynes JM, Van Ranst M, Calisher CH. Clinical characteristics of ratborne seoul hantavirus disease. *Emerg. Infect. Dis.* 25(2), 387–388 (2019).
14. Hörling J, Lundkvist Å, Jaarola M, *et al.* Distribution and genetic heterogeneity of Puumala virus in Sweden. *J. Gen. Virol.* 77(10), 2555–2562 (1996).
15. Knust B, Rollin PE. Twenty year summary of Hantavirus cases in the USA. *Emerg. Infect. Dis.* 19(12), 1934–1937 (2013).
16. Hook CJ Van, Malone R. Hantavirus Pulmonary Syndrome — The 25th Anniversary of the Four Corners Outbreak. 24(11) (2018).
17. Torrez-Martinez N, Bharadwaj M, Goade D, *et al.* Bayou Virus-Associated Hantavirus Pulmonary Syndrome in Eastern Texas : Identification of the Rice Rat , Oryzomys palustris , as Reservoir Host. *Emerg. Infect. Dis.* 4(1), 105–111 (1998).
18. Williams JR, Bryan RT, Mills JN, *et al.* AN OUTBREAK OF HANTAVIRUS PULMONARY SYNDROME IN WESTERN PARAGUAY. *Am. J. Trop. Med.*

Hyg. 57(December 1993), 274–282 (1997).

19. Pascale JM, Dragoo JW, Armien B, Nelson R, Can R. Confirmation of Choclo Virus as the Cause of Hantavirus Cardiopulmonary Syndrome and High Serum Antibody Prevalence in Panama. 1593(May), 1586–1593 (2010).
20. Peters CJ, Khan AS. Hantavirus Pulmonary Syndrome: The New American Hemorrhagic Fever. *Clin. Infect. Dis.* 34(9), 1224–1231 (2002).
21. de Oliveira RC, Guterres A, Fernandes J, D'Andrea PS, Bonvicino CR, de Lemos ERS. Hantavirus reservoirs: Current status with an emphasis on data from Brazil. Viruses6(5), 1929–1973 (2014).
22. Moolenaar RL, Dalton C, Lipman HB, *et al.* Clinical Features That Differentiate Hantavirus Pulmonary Syndrome from Three Other Acute Respiratory Illnesses Breiman Published by : Oxford University Press Stable URL : https://www.jstor.org/stable/4458882 Clinical Features That Differentiate Hantaviru. (2019).
23. Butler JC, Peters CJ. STATE-OF-THE-ART CLINICAL ARTICLE Hantaviruses and Hantavirus Pulmonary Syndrome. (June), 387–395 (1994).
24. Holmes EC, Zhang YZ. The evolution and emergence of hantaviruses. *Curr. Opin. Virol.* [Internet]. 10(L), 27–33 (2015). Available from: http://dx.doi.org/10.1016/j.coviro.2014.12.007.
25. Bennett SN, Gu SH, Kang HJ, Arai S, Yanagihara R. Reconstructing the evolutionary origins and phylogeography of hantaviruses. *Trends Microbiol.* [Internet]. 22(8), 473–482 (2014). Available from: http://dx.doi.org/10.1016/j.tim.2014.04.008.

26. Yanagihara R, Gu SH, Arai S, Kang HJ, Song JW. Hantaviruses: Rediscovery and new beginnings. *Virus Res.* [Internet]. 187, 6–14 (2014). Available from: http://dx.doi.org/10.1016/j.virusres.2013.12.038.

27. Kittelberger R. Novel prion protein in BSE-affected cattle, Switzerland. Emerg. Infect. Dis.18(5), 890–892 (2012).

28. Medina RA, Torres-Perez F, Galeno H, *et al.* Ecology, Genetic Diversity, and Phylogeographic Structure of Andes Virus in Humans and Rodents in Chile. *J. Virol.* 83(6), 2446–2459 (2009).

29. López N, Padula P, Rossi C, Lázaro ME, Franze-Fernández MT. Genetic identification of a new hantavirus causing severe pulmonary syndrome in Argentina. *Virology*. 220(1), 223–226 (1996).

30. Martinez-Valdebenito C, Calvo M, Vial C, *et al.* Person-to-person household and nosocomial transmission of andes hantavirus, Southern Chile, 2011. *Emerg. Infect. Dis.* 20(10), 1629–1636 (2014).

31. Cruz CD, Forshey BM, Vallejo E, *et al.* Novel strain of Andes virus associated with fatal human infection, central Bolivia. *Emerg. Infect. Dis.* 18(5), 750–757 (2012).

32. Padula PJ, Edelstein A, Miguel SDL, Lopez NM, Rossi CM, Rabinovich RD. Hantavirus pulmonary syndrome outbreak in Argentina: Molecular evidence for person-to-person transmission of Andes virus. *Virology*. 241(2), 323–330 (1998).

33. Toro J, Vega JD, Khan AS, *et al.* An outbreak of hantavirus pulmonary syndrome, Chile, 1997. *Emerg. Infect. Dis.* 4(4), 687–694 (1998).

34. Galeno H, Mora J, Villagra E, *et al.* First human isolate of hantavirus (Andes

virus) in the Americas. *Emerg. Infect. Dis.* 8(7), 657–661 (2002).

35. Jiang H, Du H, Wang LM, Wang PZ, Bai XF. Hemorrhagic Fever with Renal Syndrome: Pathogenesis and Clinical Picture. *Front. Cell. Infect. Microbiol.* [Internet]. 6 (2016). Available from: http://journal.frontiersin.org/Article/10.3389/fcimb.2016.00001/abstract.

36. Figueiredo LTM, Souza WM de, Ferrés M, Enria DA. Hantaviruses and cardiopulmonary syndrome in South America. *Virus Res.* [Internet]. 187, 43–54 (2014). Available from: http://dx.doi.org/10.1016/j.virusres.2014.01.015.

37. Muyangwa M, Martynova E V., Khaiboullina SF, Morzunov SP, Rizvanov AA. Hantaviral proteins: Structure, functions, and role in hantavirus infection. *Front. Microbiol.* 6(NOV), 1–10 (2015).

38. Vaheri A, Strandin T, Hepojoki J, *et al.* Uncovering the mysteries of hantavirus infections. *Nat. Rev. Microbiol.* [Internet]. 11(8), 539–550 (2013). Available from: http://dx.doi.org/10.1038/nrmicro3066.

39. Vera-Otarola J, Solis L, Soto-Rifo R, *et al.* The Andes Hantavirus NSs Protein Is Expressed from the Viral Small mRNA by a Leaky Scanning Mechanism. *J. Virol.* 86(4), 2176–2187 (2012).

40. Muranyi W, Bahr U, Zeier M, Van Der Woude FJ. Hantavirus Infection. *J. Am. Soc. Nephrol.* 16, 3669–3679 (2005).

41. Hepojoki J, Strandin T, Lankinen H, Vaheri A. Hantavirus structure - Molecular interactions behind the scene. *J. Gen. Virol.* 93(8), 1631–1644 (2012).

42. Klingström J, Åkerström S, Hardestam J, *et al.* Nitric oxide and peroxynitrite have different antiviral effects against hantavirus replication and free mature virions.

Eur. J. Immunol. 36(10), 2649–2657 (2006).

43. Simmons JH, Riley LK. Hantaviruses: An Overview. *Comp. Med.* 52(2), 97–110 (2002).

44. Jangra RK, Herbert AS, Li R, *et al.* Protocadherin-1 is essential for cell entry by New World hantaviruses. *Nature* [Internet]. 563(7732), 559–563 (2018). Available from: http://dx.doi.org/10.1038/s41586-018-0702-1.

45. Hussein ITM, Cheng E, Ganaie SS, *et al.* Autophagic Clearance of Sin Nombre Hantavirus Glycoprotein Gn Promotes Virus Replication in Cells. *J. Virol.* 86(14), 7520–7529 (2012).

46. Cifuentes-Muñoz N, Salazar-Quiroz N, Tischler ND. Hantavirus Gn and Gc envelope glycoproteins: Key structural units for virus cell entry and virus assembly. Viruses6(4), 1801–1822 (2014).

47. Smego RA, Sarwari AR, Siddiqui AR. Crimean-Congo Hemorrhagic Fever: Prevention and Control Limitations in a Resource-Poor Country. *Clin. Infect. Dis.* 38(12), 1731–1735 (2004).

48. Rachel M. Wells, Sergio Sosa Estani, Zaida E. Yadon, Delia Enria, Paula Padula, Noemi Pini, James N. Mills, Clarence J. Peters ELS. An unusual outbreak of Andes transmission. *Emerg. Infect. Dis.* 3(2), 171–174 (1997).

49. Chaparro J, Vega J, Terry W, *et al.* Assessment of person-to-person transmission of hantavirus pulmonary syndrome in a Chilean hospital setting. *J. Hosp. Infect.* 40, 281–285 (1998).

50. Martinez VP, Bellomo C, San Juan J, *et al.* Person-to-person transmission of Andes virus. *Emerg. Infect. Dis.* 11(12), 1848–1853 (2005).

51. Ermonval M, Baychelier F, Tordo N. What do we know about how hantaviruses interact with their different hosts? Viruses8(223), 1–17 (2016).

52. Hepojoki J, Vaheri A, Strandin T. The fundamental role of endothelial cells in hantavirus pathogenesis. *Front. Microbiol.* 5(727), 1–7 (2014).

53. Hammerbeck CD, Hooper JW. T Cells Are Not Required for Pathogenesis in the Syrian Hamster Model of Hantavirus Pulmonary Syndrome. *J. Virol.* 85(19), 9929–9944 (2011).

54. Godoy P, Marsac D, Stefas E, *et al.* Andes Virus Antigens Are Shed in Urine of Patients with Acute Hantavirus Cardiopulmonary Syndrome. *J. Virol.* 83(10), 5046–5055 (2009).

55. Ferrara N. Role of vascular endothelial growth factor in regulation of physiological angiogenesis. *Am. J. Physiol. - Cell Physiol.* 280, 1358–1366 (2001).

56. Borges AA, Campos GM, Moreli ML, *et al.* Hantavirus cardiopulmonary syndrome: immune response and pathogenesis. Microbes Infect.8(8), 2324–2330 (2006).

57. Gross RH, Lublin F. Interferon β in Multiple Sclerosis: A Review. *Transl. Neuroimmunol. Mult. Scler.* [Internet]. , 191–201 (2016). Available from: https://www.sciencedirect.com/science/article/pii/B9780128019146000167?via%3Dihub.

58. Charbonnel N, Pagès M, Sironen T, *et al.* Immunogenetic Factors Affecting Susceptibility of Humans and Rodents to Hantaviruses and the Clinical Course of Hantaviral Disease in Humans. *Viruses*. 6(5), 2214–2241 (2014).

59. Sargianou M, Watson DC, Chra P, *et al.* Hantavirus infections for the clinician:

From case presentation to diagnosis and treatment. *Crit. Rev. Microbiol.* 38(4), 317–329 (2012).

60. Drebot M, Jones S, Grolla A, *et al.* Hantavirus pulmonary syndrome in Canada: An overview of clinical and diagnostic features, epidemiology and prevention. *Canada Commun. Dis. Rep.* 41(6), 124–131 (2015).

61. Szabó R. Antiviral therapy and prevention against hantavirus infections. Acta Virol.61(1), 3–12 (2017).

62. Schmaljohn CS. Vaccines for hantaviruses: Progress and issues. *Expert Rev. Vaccines*. 11(5), 511–513 (2012).

63. Brocato RL, Hooper JW. Progress on the Prevention and Treatment of Hantavirus Disease. *Viruses*. 11(7), 610 (2019).

64. Cho HW, Howard CR. Antibody responses in humans to an inactivated hantavirus vaccine (Hantavax®). *Vaccine*. 17(20–21), 2569–2575 (1999).

65. Hooper JW, Josleyn M, Ballantyne J, Brocato R. A novel Sin Nombre virus DNA vaccine and its inclusion in a candidate pan-hantavirus vaccine against hantavirus pulmonary syndrome (HPS) and hemorrhagic fever with renal syndrome (HFRS). *Vaccine*. 31(40), 4314–4321 (2013).

66. Brown KS, Safronetz D, Marzi A, Ebihara H, Feldmann H. Vesicular Stomatitis Virus-Based Vaccine Protects Hamsters against Lethal Challenge with Andes Virus. *J. Virol.* 85(23), 12781–12791 (2011).

67. Custer DM, Thompson E, Schmaljohn CS, Ksiazek TG, Hooper JW. Active and Passive Vaccination against Hantavirus Pulmonary Syndrome with Andes Virus M Genome Segment-Based DNA Vaccine. *J. Virol.* 77(18), 9894–9905 (2003).

68. Ogg M, Jonsson CB, Camp J V., Hooper JW. Ribavirin protects Syrian hamsters against lethal hantavirus pulmonary syndrome - After intranasal exposure to andes virus. *Viruses*. 5(11), 2704–2720 (2013).

69. Jonsson CB, Hooper J, Mertz G. Treatment of hantavirus pulmonary syndrome. *Antiviral Res.* 78(1), 162–169 (2008).

70. Moreli ML, Marques-Silva AC, Pimentel VA, da Costa VG. Effectiveness of the ribavirin in treatment of hantavirus infections in the Americas and Eurasia: a meta-analysis. *VirusDisease*. 25(3), 385–389 (2014).

71. Bharadwaj M, Nofchissey R, Goade D, Koster F, Hjelle B. Humoral Immune Responses in the Hantavirus Cardiopulmonary Syndrome. *J. Infect. Dis.* 182(1), 43–48 (2000).

72. Brocato R, Josleyn M, Ballantyne J, Vial P, Hooper JW. DNA vaccine-generated duck polyclonal antibodies as a postexposure prophylactic to prevent hantavirus pulmonary syndrome (HPS). *PLoS One*. 7(4) (2012).

73. Hooper JW, Ferro AM, Wahl-Jensen V. Immune Serum Produced by DNA Vaccination Protects Hamsters against Lethal Respiratory Challenge with Andes Virus. *J. Virol.* 82(3), 1332–1338 (2008).

74. Garrido JL, Presscott J, Calvo M, *et al.* Two recombinant human monoclonal antibodies that protect against lethal Andes hantavirus infection in vivo. *Sci. Transl. Med.* 10(468) (2018).

75. Hooper JW, Brocato RL, Kwilas SA, *et al.* DNA vaccine-derived human IgG produced in transchromosomal bovines protect in lethal models of hantavirus pulmonary syndrome. *Sci. Transl. Med.* 6(264) (2014).

76. Schroeder HW, Cavacini L. Structure and function of immunoglobulins. *J. Allergy Clin. Immunol.* [Internet]. 125(2), S41–S52 (2010). Available from: https://linkinghub.elsevier.com/retrieve/pii/S0091674909014651.

77. Vidarsson G, Dekkers G, Rispens T. IgG subclasses and allotypes: From structure to effector functions. *Front. Immunol.* 5(520), 1–17 (2014).

78. Panda S, Ding JL. Natural Antibodies Bridge Innate and Adaptive Immunity. *J. Immunol.* 194(1), 13–20 (2015).

79. Oettgen HC. Fifty years later: Emerging functions of IgE antibodies in host defense, immune regulation, and allergic diseases. J. Allergy Clin. Immunol.137(6), 1631–1645 (2016).

80. Charles A Janeway, Jr, Paul Travers, Mark Walport and MJS. Immunobiology: The Immune System in Health and Disease. 5th ed. Garland Publishing, New York City.

81. Di Noia JM, Neuberger MS. Molecular Mechanisms of Antibody Somatic Hypermutation. *Annu. Rev. Biochem.* 76(1), 1–22 (2007).

82. Hammerbeck CD, Wahl-Jensen V, Hooper JW. Hantavirus. In: *Vaccines for Biodefense and Emerging and Neglected Diseases*, 379–411 (2009).

83. Ravetch J V, Bolland S. IGG FC RECEPTORS. *Annu. Rev. Immunol.* [Internet]. 19, 275–290 (2001). Available from: www.annualreviews.org.

84. Anderson CL. Human IgG Fc Receptors. .

85. Harmsen MM, De Haard HJ. Properties, production, and applications of camelid single-domain antibody fragments. *Appl. Microbiol. Biotechnol.* 77, 13–22 (2007).

86. Saerens D, Muyldermans S. Overview of Single Domain Antibodies [Internet]. In:

Single Domain Antibodies Methods and Protocols, 1–573 (2012). Available from: http://www.springer.com/series/7651.

87. Muyldermans S, Baral TN, Retamozzo VC, *et al.* Camelid immunoglobulins and nanobody technology. *Vet. Immunol. Immunopathol.* 128(1–3), 178–183 (2009).

88. Muyldermans S. Nanobodies: Natural Single-Domain Antibodies. *Annu. Rev. Biochem.* [Internet]. 82(1), 775–797 (2013). Available from: http://www.annualreviews.org/doi/10.1146/annurev-biochem-063011-092449.

89. Hamers-Casterman C, Atarhouch T, Muyldermans S, *et al.* Naturally occurring antibodies devoid of light chains. *Nature*. 363, 446–448 (1993).

90. Maass DR, Sepulveda J, Pernthaner A, Shoemaker CB. Alpaca (Lama pacos) as a convenient source of recombinant camelid heavy chain antibodies (VHHs). *J. Immunol. Methods*. 324(1), 13–25 (2007).

91. Daley LP, Kutzler MA, Bennett BW, Smith MC, Glaser AL, Appleton JA. Effector functions of camelid heavy-chain antibodies in immunity to West Nile virus. *Clin. Vaccine Immunol.* 17(2), 239–246 (2010).

92. Power UF, Stortelers C, Allosery K, *et al.* Generation and Characterization of ALX-0171 , a Potent Novel Therapeutic Nanobody for the Treatment of Respiratory Syncytial Virus Infection. *Antimicrob. Agents Chemother.* 60(1), 6–13 (2016).

93. Griffiths C, Drews SJ, Marchant DJ. Respiratory syncytial virus: Infection, detection, and new options for prevention and treatment. *Clin. Microbiol. Rev.* 30(1), 277–319 (2017).

94. Schepens B, Ibañez LI, De Baets S, *et al.* Nanobodies® specific for respiratory

syncytial virus fusion protein protect against infection by inhibition of fusion. *J. Infect. Dis.* 204(11), 1692–1701 (2011).

95. Raj VS, Okba NMA, Gutierrez-Alvarez J, *et al.* Chimeric camel/human heavy-chain antibodies protect against MERS-CoV infection. *Sci. Adv.* 4(8) (2018).

96. Laursen NS, Friesen RHE, Zhu X, *et al.* Universal protection against influenza infection by a multidomain antibody to influenza hemagglutinin. *Science (80-.).* 362(6414), 598–602 (2018).

97. Fatima A, Wang H, Kang K, *et al.* Development of VHH antibodies against dengue virus type 2 NS1 and comparison with monoclonal antibodies for use in immunological diagnosis. *PLoS One*. 9(4) (2014).

98. Wilken L, McPherson A. Application of camelid heavy-chain variable domains (VHHs) in prevention and treatment of bacterial and viral infections. *Int. Rev. Immunol.* [Internet]. 37(1), 69–76 (2018). Available from: https://doi.org/10.1080/08830185.2017.1397657.

99. Péchiné S, Janoir C, Collignon A. Emerging monoclonal antibodies against Clostridium difficile infection. *Expert Opin. Biol. Ther.* [Internet]. 17(4), 415–427 (2017). Available from: http://dx.doi.org/10.1080/14712598.2017.1300655.

100. Stijlemans B, Baetselier P De, Caljon G, Van Den Abbeele J, Van Ginderachter JA, Magez S. Nanobodies As tools to Understand, diagnose, and treat African trypanosomiasis. Front. Immunol.8(JUN) (2017).

101. Thys B, Schotte L, Muyldermans S, Wernery U, Hassanzadeh-Ghassabeh G, Rombaut B. In vitro antiviral activity of single domain antibody fragments against poliovirus. *Antiviral Res.* 87(2), 257–264 (2010).

102. Jähnichen S, Blanchetot C, Maussang D, *et al.* CXCR4 nanobodies (VHH-based single variable domains) potently inhibit chemotaxis and HIV-1 replication and mobilize stem cells. *Proc. Natl. Acad. Sci. U. S. A.* 107(47), 20565–20570 (2010).

103. Fridy PC, Li Y, Keegan S, *et al.* A robust pipeline for rapid production of versatile nanobody repertoires. *Nat. Methods*. (2014).

104. Brown KS, Safronetz D, Marzi A, Ebihara H, Feldmann H. Vesicular Stomatitis Virus-Based Vaccine Protects Hamsters against Lethal Challenge with Andes Virus. *J. Virol.* 85(23), 12781–12791 (2011).

105. Jiang D-B, Zhang J-P, Cheng L-F, *et al.* Hantavirus Gc induces long-term immune protection via LAMP-targeting DNA vaccine strategy. *Antiviral Res.* [Internet]. 150, 174–182 (2018). Available from: https://www.sciencedirect.com/science/article/pii/S0166354217307052?via%3Dihub.

106. Yusufu M, Shalitanati A, Yu H, *et al.* Immune responses in mice induced by multi-epitope DNA vaccine and protein vaccine of Crimean-Congo Hemorrhagic Fever Virus. *bioRxiv* [Internet]. , 719724 (2019). Available from: https://www.biorxiv.org/content/10.1101/719724v1.

107. Williams J. Vector Design for Improved DNA Vaccine Efficacy, Safety and Production. *Vaccines*. 1(3), 225–249 (2013).

108. Kutzler MA, Kraynyak KA, Nagle SJ, *et al.* Plasmids encoding the mucosal chemokines CCL27 and CCL28 are effective adjuvants in eliciting antigen-specific immunity in vivo. *Gene Ther.* 17(1), 72–82 (2010).

109. Zhang Z, Li Y, Wang M, *et al.* Immune protection of rhoptry protein 21 (ROP21)

of Toxoplasma gondii as a DNA vaccine against toxoplasmosis. *Front. Microbiol.* 9(MAY), 1–10 (2018).

110. Page M, Thorpe R. Purification of IgG using Protein A or Protein G. In: *The Protein Protocols Handbook* (2002).

111. Nunes-Silva S, Gangnard S, Vidal M, *et al.* Llama immunization with full-length VAR2CSA generates cross-reactive and inhibitory single-domain antibodies against the DBL1X domain. *Sci. Rep.* 4, 1–9 (2014).

112. Ema Romao, Francisco Morales-Yanez, Yaozhong Hu, *et al.* Identification of Useful Nanobodies by Phage Display of Immune Single Domain Libraries Derived from Camelid Heavy Chain Antibodies. *Curr. Pharm. Des.* 22(43) (2016).

113. De Vlieger D, Ballegeer M, Rossey I, Schepens B, Saelens X. Single-Domain Antibodies and Their Formatting to Combat Viral Infections. *Antibodies*. 8(1), 1 (2018).

114. Vanlandschoot P, Stortelers C, Beirnaert E, *et al.* Nanobodies¯: New ammunition to battle viruses. *Antiviral Res.* 92(3), 389–407 (2011).

115. Fridy PC, Li Y, Keegan S, *et al.* A robust pipeline for rapid production of versatile nanobody repertoires. *Nat. Methods*. (2014).

116. Haddad M, Soukkarieh C, Khalaf HE, Abbady AQ. Purification of polyclonal IgG specific for Camelid's antibodies and their recombinant nanobodies. *Open Life Sci.* (2016).

117. Terryn S, Francart A, Lamoral S, *et al.* Protective effect of different anti-rabies virus VHH constructs against rabies disease in mice. *PLoS One*. 9(10) (2014).

118. Clem AS. Fundamentals of Vaccine Immunology. *J. Glob. Infect. Dis.* 3(1), 73–78

(2011).

119. Baron S, Klimpel GR. Immune Defenses. In: *Medical Microbiology* (1996).

120. Cifuentes-Muñoz N, Salazar-Quiroz N, Tischler ND. Hantavirus Gn and Gc envelope glycoproteins: Key structural units for virus cell entry and virus assembly. *Viruses*. 6(4), 1801–1822 (2014).

121. Selcuk Unal E, Zhao R, Qiu A, Goldman ID. N-linked glycosylation and its impact on the electrophoretic mobility and function of the human proton-coupled folate transporter (HsPCFT). *Biochim. Biophys. Acta - Biomembr.* 1778(6), 1407–1414 (2008).

122. Slifka MK, Amanna I. How advances in immunology provide insight into improving vaccine efficacy. *Vaccine*. 32(25), 2948–2957 (2014).

123. Brynjolfsson SF, Henneken M, Bjarnarson SP, Mori E, Del Giudice G, Jonsdottir I. Hyporesponsiveness following booster immunization with bacterial polysaccharides is caused by apoptosis of memory B cells. *J. Infect. Dis.* 205(3), 422–430 (2012).

124. Sallusto F, Lanzavecchia A, Araki K, Ahmen R. From Vaccines to Memory and Back. *Immunity*. 33(4), 451–463 (2010).

125. Lee CW, Senne DA, Suarez DL. Development and application of reference antisera against 15 hemagglutinin subtypes of influenza virus by DNA vaccination of chickens. *Clin. Vaccine Immunol.* 13(3), 395–402 (2006).

126. Bjarnarson SP, Benonisson H, Del Giudice G, Jonsdottir I. Pneumococcal Polysaccharide Abrogates Conjugate-Induced Germinal Center Reaction and Depletes Antibody Secreting Cell Pool, Causing Hyporesponsiveness. *PLoS One*.

8(9) (2013).

127. Thompson MK, Fridy PC, Keegan S, Chait BT, Fenyö D, Rout MP. Optimizing selection of large animals for antibody production by screening immune response to standard vaccines. *J. Immunol. Methods*. 430, 56–60 (2016).

128. Safronetz D, Ebihara H, Feldmann H, Hooper JW. The Syrian hamster model of hantavirus pulmonary syndrome. *Antiviral Res.* [Internet]. 95(3), 282–292 (2012). Available from: http://dx.doi.org/10.1016/j.antiviral.2012.06.002.

129. Jiang H, Zheng X, Wang L, Du H, Wang P, Bai X. Hantavirus infection: a global zoonotic challenge. Virol. Sin.32(1), 32–43 (2017).

130. MacNeil A, Nichol ST, Spiropoulou CF. Hantavirus pulmonary syndrome. Virus Res.162(1–2), 138–147 (2011).

131. Hoey RJ, Eom H, Horn JR. Structure and development of single domain antibodies as modules for therapeutics and diagnostics. *Exp. Biol. Med.* 244(17), 1568–1576 (2019).

132. Jovčevska I, Muyldermans S. The Therapeutic Potential of Nanobodies. *BioDrugs* [Internet]. 34(1), 11–26 (2019). Available from: https://doi.org/10.1007/s40259-019-00392-z.

133. Van Heeke G, Allosery K, De Brabandere V, De Smedt T, Detalle L, de Fougerolles A. Nanobodies® as inhaled biotherapeutics for lung diseases. *Pharmacol. Ther.* [Internet]. 169, 47–56 (2017). Available from: http://dx.doi.org/10.1016/j.pharmthera.2016.06.012.